Integrating HLA and HPA in Precision Transfusion: Insights from Platelet Transfusion Refractoriness Driven by Anti-CD36 Alloimmunization and Multifactorial Hemostatic Complications

Shin-Yi Tsai

stsai22@jhu.edu

1. Department of Medicine, MacKay Medical University, New Taipei City, Taiwan; 2. Institute of Biomedical Sciences, MacKay Medical University, New Taipei, Taiwan; 3. Department of Laboratory Medicine, MacKay Memorial Hospital, Taipei City, Taiwan; 4. Department of Health Policy and Management, Johns Hopkins Bloomberg School of Public Health, Johns Hopkins University, Baltimore, MD, USA https://orcid.org/0000-0001-7978-778X

Kuan-Hsiao Lin

Taipei Blood Center, Taiwan Blood Service Foundation

Sheng-Mou Hou

Taiwan Blood Services Foundation

Research Article

Keywords: CD36 deficiency, CD36 alloimmunization, platelet transfusion refractoriness, Monoclonal Antibody-specific Immobilization of Platelet Antigens(MAIPA), Solid Phase Red Cell Adherence Assay(SPRCA)

Posted Date: September 30th, 2025

DOI: https://doi.org/10.21203/rs.3.rs-7551923/v2

Additional Declarations: The authors declare no competing interests.

Integrating HLA and HPA in Precision Transfusion: Insights from Platelet Transfusion Refractoriness Driven by Anti-CD36 Alloimmunization and Multifactorial Hemostatic Complications

Shin-Yi Tsai[1234*], Kuan-Hsiao Lin[5], and Sheng-Mou Hou[6*]

[1]Department of Medicine, MacKay Medical University, New Taipei City, Taiwan

[2]Institute of Biomedical Sciences, MacKay Medical University, New Taipei, Taiwan

[3]Department of Laboratory Medicine, MacKay Memorial Hospital, Taipei City, Taiwan

[4]Department of Health Policy and Management, Johns Hopkins Bloomberg School of Public Health, Johns Hopkins University, Baltimore, MD, USA

[5]Taipei Blood Center, Taiwan Blood Service Foundation

[6]Taiwan Blood Services Foundation

* Correspondences: Dr Shin-Yi Tsai (stsai22@jhu.edu)

Data Sharing Statement

All data supporting the findings of this study will be made available upon reasonable request to the corresponding author. Renewable materials (e.g., antibodies, plasmids, and assay protocols) will be shared without undue restriction, consistent with institutional and funding policies.

Public repository deposition (required for sequencing/omics):

Not applicable — no high-throughput sequencing or omics datasets were generated in

this study. Clinical and laboratory datasets derived from the patient cohort are available upon request, subject to institutional IRB approval and data privacy regulations. If overlapping data have been reported elsewhere, this will be clearly referenced and appropriately cited in the manuscript.

Abstract

Background: CD36, recently recognized as a distinct blood group system, encodes a class-B scavenger receptor involved in hemostasis and innate immunity. Anti-CD36 alloantibodies are an often-overlooked cause of platelet transfusion refractoriness (PTR), fetal–neonatal alloimmune thrombocytopenia (FNAIT), and bleeding disorders. Although newer assays are available, the relative effectiveness of platelet antibody tests remains uncertain. We review the clinical features of CD36 deficiency and alloimmunization, compare the Solid Phase Red Cell Adherence Assay (SPRCA) with ELISA for antibody detection, and propose a streamlined diagnostic algorithm for PTR.

Materials and Methods: A retrospective cohort study was conducted at a tertiary center over 6.5 years, involving 2,333 patients who underwent platelet antibody testing. Antibody screening used parallel SPRCA and qualitative solid-phase ELISA, with confirmatory tests including MAIPA, molecular genotyping, and flow cytometry

for CD36 antigen expression. Six illustrative cases with genetically or phenotypically confirmed CD36 deficiency were examined in detail.

Results: ELISA detected antiplatelet antibodies in 33.6% of samples, while SPRCA detected them in 18.7%, with an overall concordance of 78.2% ($\kappa = 0.451$). ELISA identified additional antibodies in 18.4% of cases, whereas SPRCA alone detected 3.4%. Dual positivity strongly indicates pathogenic alloantibodies responsible for transfusion refractoriness.

Conclusions: CD36 deficiency poses a significant immunohematologic challenge in PTR and FNAIT. Employing both ELISA and SPRCA for screening, along with reflex confirmatory testing, improves diagnostic accuracy for anti-CD36 alloimmunization, enhances transfusion strategies with CD36-negative platelet transfusions, and increases patient safety. Establishing rare donor registries is crucial for providing personalized transfusion support to affected individuals.

Introduction

CD36 (glycoprotein IV) is a heavily N-glycosylated class-B scavenger receptor expressed on platelets, monocytes, endothelium, and erythroid lineage cells[1,2]. Early studies defined the Naka– (CD36-negative) phenotype[3] and established type I and type II deficiency (absent on platelets±monocytes)[4], providing the immunohematologic framework for today's diagnostics[5]. Its polymorphic expression

on red cells and null variants, now recognized by The International Society of Blood Transfusion supports classifying CD36 as a blood group system with clear. clinical relevance[6,7]. Anti-CD36 is an important, often under-recognized cause of FNAIT[8,9,10] and fetal anemia[6,11], demonstrating effective prenatal therapy in preclinical models and editorially highlighting integration into perinatal workflows.[12] Mechanistically, platelet CD36 surface density correlates with prothrombotic signaling responses[12,13] (e.g., to oxidized low-density lipoprotein)[14,15], helping to explain why deficiency or alloimmunization can materially alter hemostasis[16]. In transfusion practice, anti-CD36–mediated platelet transfusion refractoriness (PTR)[17,18], which should be considered when Human Leukocyte Antigen and Human Platelet Antigen (HLA/HPA) matching fails[18], especially in high-prevalence populations[5], and may contribute to post-transfusion purpura (PTP)[19,20]. Finally, flow cytometry remains first-line for phenotyping[5,21], while optimized Monoclonal Antibody-specific Immobilization of Platelet Antigens (MAIPA) capture clones (GZ-70/GZ-608) markedly improve anti-CD36 detection over legacy reagents, enabling more reliable case identification and targeted donor selection[22].

CD36 deficiency exhibits notable geographic differences, affecting 2–4% of Chinese[23,24] populations, 3%-11% of Japanese[3] populations, 2.6% of Middle Eastern[25] populations, and up to 3% of African[26,27] populations, but remains rare(<0.4%) in

Europeans, which explains the low rate of anti-CD36 alloimmunization in Western populations.

Recent advancements in high-throughput sandwich Enzyme-Linked Immunosorbent Assay (ELISA) have surpassed conventional methods for CD36 phenotyping, achieving intra- and inter-assay variations as low as 2.1–5.2%[23]. Diagnosis remains challenging due to the disorder's rarity and the need for multiplexed approaches beyond standard antibody screens, especially in patients with comorbidities that can mask or mimic clinical features. Accurate diagnosis depends on comprehensive tests, including flow cytometry[28], MAIPA[29], Solid Phase Red Cell Adherence Assay (SPRCA), ELISA, and molecular genotyping, to distinguish CD36-related platelet alloimmunization from other causes. Our clinical series underscores the importance of integrated diagnostics for accurate identification in complex hemostatic disorders and guides optimal transfusion management.

Accurate detection of antiplatelet antibodies is essential in managing Immune Thrombocytopenia, FNAIT, and PTR. At MacKay Memorial Hospital (MMH), since 2019, parallel testing using SPRCA and PAKPLUS® ELISA has revealed a persistent "gray zone" of detection discrepancies[30]. Integrating CD36 antigen typing and anti-

CD36 antibody screening has been pivotal for elucidating PTR mechanisms, highlighting the need for standardized thresholds to improve diagnostic precision.

Patients and methods

We would report that patients, including cases 1[31], 2-4[30], 5, and 6[32], have CD36 deficiency and CD36-related refractoriness.

Case 1: A 78-year-old female patient with lung adenocarcinoma and a documented CD36 deficiency was admitted with respiratory distress caused by pneumonia. Initial treatment involved empiric antibiotics, notably teicoplanin (400 mg IV daily), administered from January 30 to February 7 and resumed on February 25. Piperacillin/tazobactam was given concurrently from January 30 to February 6. Meropenem was initiated on February 4 and continued until the patient's death. Ceftriaxone was added to the antimicrobial regimen from February 18 to February 25.

Case 2 was a 32-year-old pregnant woman. Case 3 was a 60-year-old man with metastatic small-cell carcinoma, Sjögren's syndrome, and an unexpected PTR. Case 4 was a 21-year-old woman with acute leukemia, cellulitis, disseminated intravascular coagulation (DIC), and PTR. Case 5 was a 46-year-old man with severe cardiovascular disease, ischemic gangrene requiring multiple amputations, acute respiratory failure, and repeated surgical interventions. Case 6 was an 86-year-old

woman with chronic lymphoma, recurrent infections, dementia, chronic heart failure, and atrial fibrillation.

Additionally, our retrospective 6.5-year analysis of 2,333 samples tested using SPRCA and ELISA under standardized protocols at MMH from January 2019 to June 2025 found that positive results from either method prompted clinical interpretation. Discrepancies were categorized as either concordant (positive/negative) or discordant (ELISA-only/SPRCA-only).

Methods

Clinical Assessment

Patients were evaluated for CD36 alloimmune risk using transfusion history, pregnancy records, platelet increment data, and pertinent clinical information.

Platelet Antibody Screening and Confirmation of Specificity

Primary detection of platelet alloantibodies, including anti-CD36, was performed using SPRCA. Wells were coated with anti-thrombocyte antibody, then incubated with PRP from 12 random donors and patient serum; indicator red blood cells were used to identify antibody binding. SPRCA was supported by MAIPA, lymphocytotoxicity test (LCT), or chloroquine-modified SPRCA when results were ambiguous.

Supplemental ELISA: PAKPLUS

The PAKPLUS ELISA (Immucor) evaluated serum reactivity against key platelet glycoproteins (GPIIb/IIIa, GPIa/IIa, GPIb/IX, GPIV/CD36, HLA) using kit controls; results were determined by measuring optical density.

Flow cytometric assessment of CD36 expression

Using fluorescence-activated cell sorting (FACS), platelet CD36 was measured after dual labeling of PRP with FITC–anti-CD36 and PerCP–anti-CD41a; 5,000 CD41a+ events were analyzed. Monocyte CD36 levels were assessed in lysed whole blood using FITC–anti-CD36 and PerCP–anti-CD14, with 2,000 CD14+ events analyzed.

Molecular typing: CD36 exon 5 sequencing

Genomic DNA was extracted from EDTA-anticoagulated blood (MagCorePlus automated platform) from two CD36-deficient samples. Exon 5 and the surrounding intronic regions of CD36 were amplified using exon-specific primers (Forward 5′-AGATCTAATGTTCACATATG-3′; Reverse 5′-GATTAATTACATGAGTTCTAG-3′). PCR cycling included 35 cycles of denaturation at 95°C for 30 seconds, annealing at 50°C for 60 seconds, and extension at 72°C for 30 seconds, followed by a final extension at 72°C for 10 minutes. Amplicons were sequenced using Sanger sequencing on an Applied Biosystems 3730xl DNA Analyzer at an external core facility, and sequence analysis followed standard bidirectional trace review with quality control of base calling.

Quality control and interpretation

All serologic assays included both kit-provided and in-house positive and negative controls; any runs that did not meet control acceptance criteria were repeated. Ambiguous serology results were clarified through orthogonal testing (chloroquine-modified SPRCA, MAIPA, and LCT) and by correlating with cellular CD36 expression and the CD36 exon 5 sequence, when available.

Results

Case 1: Clinical Presentation

During hospitalization, the patient quickly developed worsening, confluent, and prominent bilateral ecchymoses with significant soft tissue swelling on the axillae, chest, and limbs. The cutaneous surface demonstrated widespread disruptions, persistent serous exudation, and widespread macular lesions on the thigh. On February 7, she experienced an episode of acute, massive hematochezia exceeding 800 mL, along with sharp drops in both hemoglobin and platelet counts. Despite prompt transfusions of packed red blood cells, fresh frozen plasma, and pooled platelets, the cytopenia remained resistant to treatment. An urgent colonoscopy revealed a large colonic perforation, with widespread bruising observed across multiple areas.

Targeted transfusion of CD36-negative platelets caused a temporary but significant rise in platelet count (Figure 2B). Supportive care was aggressive, including broad-spectrum antimicrobials (Figure 2A), hemodialysis, and plasma exchange (Figure 1). However, hemorrhagic activity remained uncontrolled, and disseminated intravascular coagulation (DIC) worsened, leading to progressive multi-organ failure.

Laboratory Findings

Laboratory evaluation revealed significant thrombocytopenia and coagulopathy[33], including prolonged prothrombin time (PT/INR), elevated total and direct bilirubin, D-dimer, and fibrin degradation products, with low fibrinogen (Figure 2C)[34]. Haptoglobin (<30 mg/dL) indicated acute hemolysis or massive consumptive bleeding (Figure 2B). Renal and hepatic functions were impaired (Figure 1), consistent with multi-organ involvement.

Diagnostic Assessment

Considering her known CD36 deficiency and history of multiple transfusions, immunologic studies were conducted. ELISA and flow cytometry detected an anti-CD36 (anti-Naka) alloantibody. Platelets showed no expression of the CD36 antigen, and MAIPA screening confirmed the deficiency of CD36. She received a transfusion of CD36-negative platelets, which led to sustained platelet recovery by February 19.

Flow cytometric fluorescence profiles verified the absence of detectable anti-CD36 antibodies in the patient's serum (Figure 3A-C).

This presentation illustrates the clinical features of severe, resistant DIC in the context of PTR. It is characterized by catastrophic gastrointestinal bleeding, extensive skin involvement, and significant vascular damage. These dermatologic signs, such as increasing ecchymoses and blister rupture, along with widespread mucocutaneous systemic bleeding, emphasize the severity of vascular injury and widespread capillary fragility, highlighting the overlapping hemorrhagic and thrombotic disorders that characterize the final stage of PTR complicated by advanced DIC.

Since Case 2 was pregnant and diagnosed with NAITP, maternal flow cytometry clearly showed complete CD36 deficiency on platelets and monocytes, confirming maternal Type I CD36 deficiency. The paternal CD36 phenotype tested positive, establishing an antigenic incompatibility that could trigger maternal alloimmunization. (Figure 4 A-F) Additional serological tests using SPRCA assays identified maternal anti-CD36 antibodies, with IgG specifically binding to CD36-positive platelets. Crossmatch serology confirmed these findings, showing that maternal serum bound only to CD36-positive platelets without reactivity to CD36-

negative platelets. Neonatal serum showed no independent antibody activity, indicating passive transfer of maternal antibodies.

The neonate was born with severe thrombocytopenia, with an initial platelet count of $40 \times 10^3/\mu L$, presenting as petechiae. The platelet counts naturally rose to $332 \times 10^3/\mu L$ within eight days, following a recovery pattern typical of NAIT. Meanwhile, progressive anemia was observed, with hemoglobin dropping from 12.6 g/dL at birth to 9.1 g/dL by day 8; however, this anemia was not directly attributable to anti-CD36 antibodies. Additionally, intermittent episodes of neonatal desaturation occurred, likely due to perinatal stress or infection rather than antibody-mediated mechanisms.

In **Case 3**, anti-CD36 was detected using support from SPRCA, and a biallelic CD36 mutation confirmed the genetic basis of homozygosity (Figure 5E), explaining the type I CD36 deficiency. This genetic evidence validated the immunophenotypic absence of CD36 on platelets and monocytes, as shown by flow cytometry in Figures 5A-D. The patient experienced severe anemia from melena, severe thrombocytopenia (~13–15K/μL), and developed anti-CD36 alloantibodies after transfusions, which explained the persistent PTR. His cardiac and metabolic assessments revealed elevated NT-proBNP, indicating worsening cardiometabolic stress, along with hyponatremia. He also reported fatigue, chest pain, and exercise intolerance.

Case 4: Anti-CD36 was conclusively detected by SPRCA and showed absence of CD36 on platelets and monocytes assessed by flow cytometry (type I deficiency) (Figure 6A-D). Biallelic CD36 mutations confirmed the CD36 deficiency (Figure 6E). She also developed anti-CD36, resulting in severe thrombocytopenia (~15K/μL), transfusion dependence, and refractoriness to platelet support. Her cardiac issues included cardiomegaly, elevated BNP, and acute heart failure.

Case 5: The patient's clinical course was characterized by severe platelet refractoriness, starting with an initial platelet count of $27\times10^3/\mu L$. After surgery, his count rebounded significantly, reaching up to $758\times10^3/\mu L$, a response that intensified with repeated surgical stress, ischemic conditions, and systemic inflammatory reactions caused by extensive tissue necrosis. Although such fluctuations are typically indicative of consumptive coagulopathy, DIC, or reactive thrombocytosis following major surgery, recent specialized testing provides crucial clarification. Flow cytometry performed on the patient's platelets and monocytes revealed markedly reduced or absent CD36 expression, confirming the diagnosis of CD36 deficiency. (Figure 7 A-H) Additionally, serological testing detected the presence of specific anti-CD36 antibodies through MAIPA and SPRCA, confirming alloimmunization.

He exhibited a significantly elevated NT-proBNP level (1710 pg/mL), consistent with acute heart failure. The patient's history of hypertension,[11] mellitus with complications, stroke, and ARDS-induced pneumonia indicated severe cardiovascular and metabolic stress.

Case 6: The 86-year-old patient presented with thrombocytopenia primarily related to her underlying lymphoma, chronic infections, and age-related conditions, which made it difficult to definitively interpret CD36 involvement. Despite significant cardiomegaly and metabolic symptoms, typical signs directly caused by CD36 deficiency were not clear, and no anti-CD36 antibodies were detected.

Clinical Interpretation of ELISA versus SPRCA: In this cohort of 2,333 evaluations, ELISA demonstrated a higher detection rate of antiplatelet antibodies (33.6%) compared to SPRCA (18.7%). The agreement between the two methods was moderate, with an overall concordance of 78.2% and a Cohen’s kappa of 0.451, adjusting for chance. Notably, only 15.3% of all cases were concordant double-positives, while discordant results mainly involved ELISA-only positives (18.4%) versus SPRCA-only positives (3.4%). Method-specific analysis further emphasized this imbalance: 81.7% of SPRCA-positive samples were confirmed by ELISA, and nearly a quarter (22.6%) of SPRCA-negative cases were classified as positive by ELISA.

Discussion

1. Clinical relevance

The clinical vignette (Case 1) illustrates the disastrous convergence of three distinct but synergistic pathophysiological processes: anti-CD36 alloimmunization, drug-induced thrombocytopenia (DITP), and DIC[33]. DITP[35], notably linked to medications such as antibiotics, further complicates clinical management. Teicoplanin-associated DITP typically appears 5-7 days after exposure, aligning with the patient's thrombocytopenic episode and the timeline of clinical deterioration. The sequential administration of multiple broad-spectrum antibiotics, including meropenem and ceftriaxone reflects increasing concern for multidrug-resistant infections and the management of sepsis. The pathogenesis involves teicoplanin-dependent antibodies that target epitopes on GPIIb/IIIa or GPIb/V/IX complexes, leading to antibody-mediated platelet destruction.[36] Studies demonstrate a 4.6% incidence of teicoplanin-induced thrombocytopenia in clinical populations, with a median onset of 5 days and maximum platelet decrease within 8 days.

Immunological assessment, including CD36 antigen typing and anti-CD36 antibody testing, clarified that immune-mediated platelet transfusion refractoriness was caused by massive transfusions of standard random donor platelets due to the high immunogenicity of CD36 and its widespread presence on donor platelets. This likely

existed prior to sensitization and contributed to the development of anti-CD36 alloantibodies. Consequently, CD36-negative platelet transfusions are required for temporary clinical improvement. However, persistent and consumptive coagulopathy DIC significantly increased the risk of likely PTP, a massive hemorrhage caused by a "perfect storm" of etiologies and severe thrombocytopenia involving alloimmune and consumptive mechanisms. This complicated the effectiveness of supportive treatments, including infection management, coagulation correction, and targeted immunotherapy (e.g., IVIG for CD36 isoimmune PTR; platelet washing[37], leukoreduction[38], and plasma exchange, which attempted to remove antibodies[39-41]).

This scenario highlights the need for a systematic approach to severe thrombocytopenia, including the timing of drug exposures by increasing clinician awareness of DITP and promptly discontinuing the offending drug[36,42], and avoiding reexposure[43]. Additionally, it involves screening for alloantibodies, establishing registries for CD36-deficient donors, and assessing for DIC to guide appropriate therapy. Further research into treatments for PTR complicated by anti-CD36 alloimmunization and DITP is essential to improve clinical guidelines and patient outcomes. Consider reserving a compatible unit in case of bleeding risk or procedures.

Case 2: This clinical scenario underscores the urgent need to quickly identify maternal CD36 deficiency and its link to alloimmunization in neonates presenting with unexplained severe thrombocytopenia. Accurate serologic detection of anti-CD36 antibodies allows for early intervention and appropriate clinical management, potentially preventing serious neonatal complications.[11] Furthermore, differentiating NAIT from non-immune etiologies such as infections or perinatal complications is crucial for making optimal treatment decisions and accurately predicting outcomes.[10] Therefore, increased clinical awareness and involving an expert panel throughout the prenatal and postnatal stages[44,45] and conducting comprehensive serologic assessments are strongly recommended in cases suspected of alloimmune thrombocytopenia, especially those involving CD36 deficiency.

Early recognition of this anti-CD36-mediated refractoriness thrombocytopenia enables precise and restrictive transfusion strategies[46], such as selecting CD36-negative donors to source CD36-negative platelet units[47] and enhancing clinical monitoring, prophylactic measures during pregnancy, the antenatal administration of IVIG[48,49] and/or steriods[49,50], and/or deg-mAb 32-106[11], to help optimize patient outcomes and enhance transfusion safety and effectiveness. Postnatal maternal platelets for neonatal transfusion should be washed to remove HPA antibodies and irradiated to prevent GVHD[51].

Cases 3 and 4 emphasize the essential role of specialized diagnostics in managing rare platelet alloimmunization and how CD36 deficiency intersects with complex diseases, transfusion, and cardiometabolic care. Flow cytometry and sequencing confirmed CD36 deficiency, while SPRCA assays verified the causative anti-CD36 antibodies. Severe thrombocytopenia directly reflects the immunohematology impact of anti-CD36 antibodies formed caused by CD36 deficiency, which complicates underlying diseases and can worsen heart failure through impaired myocardial fatty acid metabolism[52,53], potentially increasing vulnerability to cardiac dysfunction under metabolic stress[54]. This critically impacts patient management by complicating transfusion therapy, raising the risk of PTR, and potentially aggravating cardiometabolic instability in severe underlying diseases.

Minimize Platelet Transfusion; Immunosuppression/Desensitization

In the Case 4 scenario, an AML patient has anti-CD36. The immune PTR in patients with hematologic malignancies varies widely, ranging from 7% to 34%[55]. Minimizing prophylactic platelet transfusions and transfusing only when bleeding occurs is an optimized approach to blood management[46,56]. Withholding platelet transfusions during chemotherapy-induced aplasia unless bleeding occurs can help reduce ongoing destruction of incompatible platelets[57] and limit further immune stimulation[4]. Moreover, temporary suppression of anti-CD36 production can be attempted.

Regimens have included rituximab, bortezomib[58], and plasmapheresis to remove antibodies. In one severe case, these measures only modestly lowered antibody levels (anti-CD36), with the mean fluorescence intensity falling but rebounding within days[4], underscoring that current desensitization is often inadequate. Aberrant CD36 overexpression on leukemic blasts has been linked to lower complete remission rates and early relapse**,** reflecting its involvement in chemoresistance pathways and treatment failure. Furthermore, high CD36 expression is independently associated with worse overall survival and event-free survival[59]**,** likely through altered lipid uptake, metabolic reprogramming, and enhanced leukemic persistence stem cells[59,60]. Overall, these findings position CD36 not only as a predictor of therapeutic response but also as a potential therapeutic target[61] to overcome drug resistance and improve long-term outcomes in AML patients[62].

Alternate Hemostatic Support: If platelets are ineffective, adjuncts such as antifibrinolytics or thrombopoietin mimetics may be considered, although the evidence is limited. Experimental therapies are also being explored; for example, an "effector-silencing" anti-CD36 monoclonal antibody has been proposed to block the patient's antibodies[57], thereby allowing safe transfusion.

In case 5, with severe PTR, undetected CD36 alloimmunization was the cause.[17] Specifically, despite multiple platelet transfusions, his post-transfusion counts remained near zero until an anti-CD36 isoantibody was identified, which caused rapid clearance of transfused platelets. In known CD36-deficient patients undergoing surgery or therapy, it is crucial to minimize allogeneic transfusions to prevent triggering anti-CD36 alloimmunization.

The literature on CD36 deficiency indicates complex metabolic interactions. Experimental data suggest a protective metabolic effect in CD36 deficiency[63] regarding diabetic cardiomyopathy and atherosclerosis[64,65]. However, the patient's severe phenotype underscores the multifactorial nature of cardiovascular disease, especially in chronic diabetic[54] and hypertensive contexts.[45]

CD36 plays a vital role in platelet activation and lipid metabolism and has been proposed as a therapeutic target to reduce thrombotic risk in individuals[46,64,66] with dyslipidemia. Type I CD36 deficiency is linked to atherosclerosis[67], altered glycolipid metabolism[68], and cardiomyopathy[69]. In CD36-deficient myocardium, reduced fatty acid uptake shifts energy metabolism toward glucose utilization, which consequently affects myocardial remodeling and function. Clinically, patients with type I CD36 deficiency, especially those without prior anti-CD36 alloimmunization, require

careful perioperative and transfusion management[70] due to potential metabolic and hemostatic alterations[71].

Beyond transfusion reactions, CD36 deficiency has widespread systemic effects that can impact cardiovascular health, neurological injury responses, and metabolic regulation, including decreasing diabetic cardiomyopathy and ischemia-reperfusion myocardial damage[68]. In studies of platelet function, CD36 deficiency results in slower thrombus formation[52,64,72] and CD36-null platelets are less responsive to thrombogenic stimuli like oxidized lipids, resulting in delayed clot formation on thromboelastography[33]. These findings suggest that CD36 deficiency might protect against acute ischemic events like myocardial infarction or stroke in certain situations. In fact, the absence of CD36 improved outcomes in stroke models[73], with CD36-deficient animals displaying smaller brain infarcts, better blood–brain barrier integrity, and improved functional recovery after stroke[74].

These cases underscore the vital role of advanced platelet antibody detection techniques in distinguishing CD36-related conditions from thrombocytopenia caused by other chronic diseases. The presence of severe underlying conditions, particularly lymphoma and extensive surgical trauma, significantly influences the clinical signs of CD36 deficiency. Accurate detection of anti-CD36 antibodies using MAIPA[22] and

SPRCA assays allows for the development of tailored management strategies, emphasizing the importance of high diagnostic suspicion and specialized testing in complex cases.

In contrast, as shown in Case 6 with lymphoma-related thrombocytopenia, a CD36-negative patient without alloantibodies can initially receive standard platelets without immediate destruction, because no anti-CD36 antibodies are present. However, her transfusion refractoriness likely results from non-immune factors, such as splenomegaly or HLA antibodies, rather than CD36 alloantibodies. Such a patient is at high risk of developing anti-CD36 after any transfusion. This risk justifies proactive blood management, including a restrictive transfusion policy and early antibody screening.

In summary, CD36 deficiency complicates transfusion outcomes by forming an often-overlooked immune barrier. If left unrecognized, it results in refractory thrombocytopenia, despite adequate platelet doses[75]. Once identified, clinicians should tailor transfusion support by sourcing rare donors or using immunosuppressants to prevent alloimmune destruction and employing leukoreduction, which can reduce alloimmune platelet refractoriness from 14% to 4% in patients receiving chemotherapy for acute leukemia or stem cell transplantation[38,59].

The profound refractoriness observed with anti-CD36 (Case 5) compared to standard management of thrombocytopenia without such antibodies (Case 6) underscores the clinical importance of CD36 alloimmunization in hematology. Ultimately, the immune dysregulation and metabolic effects of CD36 deficiency have major implications for cancer treatment. CD36 is a pattern-recognition scavenger receptor on monocytes, macrophages, and dendritic cells that binds danger signals (DAMPs) and pathogen components (PAMPs)[76]. It aids in phagocytosing bacteria and cell debris and modulates cytokine production during infections. CD36 is expressed in various cancer cells and immune cell subsets, where it exerts both pro- and anti-tumorigenic roles[77].

In patients with hematologic malignancies, maintaining an intact innate immune response is crucial as they are often neutropenic or lymphopenic due to chemotherapy[24]. Therefore, the optimal function of macrophages and other remaining immune cells is essential for fighting infection. CD36 deficiency can impair innate immunity, for example, by reducing macrophage uptake of Gram-negative bacteria and diminishing Toll-like receptor signaling, resulting in reduced cytokine release. This could make an immunocompromised cancer patient even more vulnerable to sepsis or fungal infections[78,79].

2. Recommended Diagnostic Strategy

Overview of Agreement Metrics and Clinical Implications

A comparative analysis of 2,333 paired samples revealed an overall agreement of 78.2% between ELISA and SPRCA, with positive and negative agreement rates of 81.7% and 77.4%, respectively. Moderate agreement ($\kappa = 0.451$) indicates that relying on a single platform may either overestimate or underestimate the alloimmunization risk, emphasizing significant assay-specific differences. Specifically, ELISA detected 18.4% more positives, likely reflecting increased sensitivity for low-affinity or non–complement–fixing antibodies of uncertain clinical relevance. Meanwhile, the 3.4% of SPRCA positives probably represent alloantibodies with higher clinical significance, consistent with SPRCA's dependence on antigen density and its lower susceptibility to nonspecific binding. These findings highlight the complementary nature of ELISA and SPRCA rather than their interchangeability. Specifically, ELISA provides broad antibody detection, while SPRCA enhances detection of functionally relevant signals. In the context of platelet transfusion refractoriness, relying on only one assay risks patient misclassification and the selection of inappropriate donors. Therefore, a sequential, tiered diagnostic approach combining high-throughput screening with ELISA, targeted confirmation with SPRCA, and molecular tools such as flow-cytometric CD36 phenotyping and

next-generation HPA/HLA genotyping[22] offers opportunities to refine antibody characterization[80], link serologic patterns with donor genetics, and ultimately improve matching strategies for highly alloimmunized patients.

GP-specific antibody assays most effectively detect anti-Nak (a). However, false negatives can occur due to monoclonal antibody interference that blocks human antibody binding.[13] Conventional platforms, such as Luminex bead assays and the MAIPA assay, often miss anti-CD36 because of epitope competition with capture antibodies (clone FA6-152). Employing ELISA for initial broad screening is recommended due to its efficiency and scalability. Subsequently, all ELISA-positive samples should be confirmed with SPRCA or other high-specificity assays, such as MAIPA[22] or flow cytometry[24], which are crucial for clinical decisions. Dual positive results on ELISA and SPRCA strongly indicate pathogenicity, while discordant cases require a detailed review of clinical and laboratory data, including transfusion history and symptoms. This integrated approach enhances the accuracy of anti-CD36 detection, supports thrombocytopenia management, and aligns with emerging evidence. Interpretation guidelines for clinical decisions should be as follows: samples positive by both ELISA and SPRCA are highly valid, indicating true positivity. Discordant results (ELISA-positive/SPRCA-negative or ELISA-negative/SPRCA-positive) should undergo further reflex testing through clinical

correlation, including a review of the transfusion history, symptoms, and other relevant laboratory results.

Overall strategies:

In practice, prevention, rapid triage, and targeted support should serve as the foundation of managing immune PTR[81]. Establish a universal pre-storage leukoreduction standard to limit HLA alloimmunization[38,82]. In cases of refractoriness, especially when HLA/HPA-matched platelets fail, use parallel SPRCA and ELISA with reflex MAIPA/flow to determine specificity (including anti-CD36) and the phenotype/genotype of CD36 (Type I/II). Transfuse to prevent antibody formation: prioritize crossmatch-compatible or HLA-matched platelets. For confirmed anti-CD36, source CD36-negative units (± HLA/HPA matching) [10,81]. When rapid intervention is clinically necessary, consider plasma exchange or immunoadsorption combined with IVIG for short-term reduction of pathogenic Fc-mediated clearance[83]. Reserve rituximab[65], and, in carefully managed rescue cases, plasma-cell–targeted therapies (e.g., bortezomib, daratumumab[84]) for high-titer, persistent cases. Finally, ensure institutional readiness by accessing CD36-negative donor registries, utilizing standardized MAIPA capture clones[22], implementing predefined reflex algorithms, and routinely monitoring CCI/bleeding outcomes[85] to support continuous quality improvement.

Acknowledgements

We sincerely thank the medical teams, the Blood Bank of MacKay Memorial Hospital, the Taipei Blood Center, and the Taiwan Blood Services Foundation for their dedicated support and expertise in transfusion medicine. Their steadfast commitment to strict standards in blood collection, testing, and specialized transfusion services was crucial to the successful completion of this study. The staff's teamwork and careful focus on both patient care and laboratory quality greatly improved the integrity of our research.

Declarations

Ethics approval and consent to participate

The Institutional Review Board(IRB) of MacKay Memorial Hospital approved this study.

When consent was obtained: Written informed consent was obtained from the patient (or the patient's legal guardian) for participation in the study and for publication of the clinical details (including any relevant images), in accordance with institutional and international ethical guidelines. When consent could not be obtained, the IRB approved a waiver of informed consent in accordance with ethical guidelines, as the study involved a retrospective analysis of de-identified clinical data and posed no more than minimal risk to participants.

Consent for publication

The authors agree with the publication of this paper.

Declaration of originality

The authors confirm that this manuscript is original and independent from other submitted or published works.

Ethics and Transparency

1. All clinical investigations were conducted under the oversight of the institutional IRB. Selected elements of this work were previously presented in abstract form at the 2024 AABB Annual Meeting and are accepted for presentation at the 2025 ISBT Regional Congress. This manuscript is currently under peer review. Updates will be reflected in subsequent versions of this preprint.
2. Some data from this patient cohort are also reported in Transfusion (2024; https://doi.org/10.1111/trf.18002), titled “P-HC-4 A Case of Platelet Transfusion Refractoriness in a CD36-Deficiency Patient with Drug-Induced Thrombocytopenia.” The present manuscript differs in its objectives and analyses, although we acknowledge partial overlap in the source population.

References

1. Hoosdally SJ, Andress EJ, Wooding C, Martin CA, Linton KJ. The Human Scavenger Receptor CD36: glycosylation status and its role in trafficking and function. *J Biol Chem*. 2009;284(24):16277-16288.

2. Martin CA, Longman E, Wooding C, et al. Cd36, a class B scavenger receptor, functions as a monomer to bind acetylated and oxidized low-density lipoproteins. *Protein Sci*. 2007;16(11):2531-2541.

3. Tomiyama Y, Take H, Ikeda H, et al. Identification of the platelet-specific alloantigen, Naka, on platelet membrane glycoprotein IV. *Blood*. 1990;75(3):684-687.

4. Pedini P, Hicheri Y, Bertand G, et al. A case of platelet transfusion refractoriness in a CD36-negative patient with acute myeloid leukemia: Diagnostic and therapeutic management. *Transfusion*. 2022;62(10):2148-2150.

5. Yamamoto N, Ikeda H, Tandon NN, et al. A platelet membrane glycoprotein (GP) deficiency in healthy blood donors: Naka- platelets lack detectable GPIV (CD36). *Blood*. 1990;76(9):1698-1703.

6. Alattar AG, Storry JR, Olsson ML. Evidence that CD36 is expressed on red blood cells and constitutes a novel blood group system of clinical importance. *Vox Sang*. 2024;119(5):496-504.

7. Storry JR, Azouzi S. An uncommon MALady: is the AnWj puzzle complete? *Blood*. 2024;144(26):2688-2689.

8. Curtis BR, Ali S, Glazier AM, Ebert DD, Aitman TJ, Aster RH. Isoimmunization against CD36 (glycoprotein IV): description of four cases of neonatal isoimmune thrombocytopenia and brief review of the literature. *Transfusion*. 2002;42(9):1173-1179.

9. Curtis BR, Ali S, Glazier AM, Ebert DD, Aitman TJ, Aster RH. Isoimmunization against CD36 (glycoprotein IV): description of four cases of neonatal isoimmune thrombocytopenia and brief review of the literature. *Transfusion*. 2002;42(9):1173-1179.

10. Stanworth SJ, Mumford AD. How I diagnose and treat neonatal thrombocytopenia. *Blood*. 2023;141(22):2685-2697.

11. Xu X, Chen D, Ye X, et al. Successful prenatal therapy for anti-CD36-mediated severe FNAIT by deglycosylated antibodies in a novel murine model. *Blood*. 2021;138(18):1757-1767.

12. Zhu W, Li W, Silverstein RL. Advanced glycation end products induce a prothrombotic phenotype in mice via interaction with platelet CD36. *Blood*. 2012;119(25):6136-6144.

13. Ruggeri ZM. Platelets in atherothrombosis. *Nature medicine*. 2002;8(11):1227-1234.

14. Yang M, Silverstein RL. CD36 signaling in vascular redox stress. *Free Radical Biology and Medicine*. 2019;136:159-171.

15. Ghosh A, Murugesan G, Chen K, et al. Platelet CD36 surface expression levels affect functional responses to oxidized LDL and are associated with inheritance of specific genetic polymorphisms. *Blood*. 2011;117(23):6355-6366.

16. Ahlen MT. Fighting anti-CD36–mediated FNAIT. *Blood*. 2021;138(18):1650-1652.

17. Sekayan T, Allen ES, Kopko P, et al. Management challenge of a rare concomitant platelet glycoprotein IV/CD36 and IIb/IIIa deficiencies: Case illustration. *Transfusion*. 2025;65(4):767-772.

18. Nahirniak S, Nadarajan V, Stanworth SJ. How I treat patients who are refractory to platelet transfusions. *Blood*. 2025;145(20):2293-2302.

19. Bierling P, Godeau B, Fromont P, et al. Posttransfusion purpura-like syndrome associated with CD36 (Naka) isoimmunization. *Transfusion*. 1995;35(9):777-782.

20. Xu X, Ye X, Xia W, et al. Studies on CD36 deficiency in South China: Two cases demonstrating the clinical impact of anti-CD36 antibodies. *Thromb Haemost*. 2013;110(6):1199-1206.

21. Cserti CM, Xu S, Sutherland R, et al. Quantitative Flow Cytometric Assessment of CD36 (Platelet Glycoprotein IV) Expression on Monocytes and Platelets: Assay Development, Role in Plasmodium falciparum Risk Assessment, and Relationship to Sickle Hemoglobin. *Blood*. 2007;110(11):3857-3857.

22. Xu X, Chen D, Ye X, et al. Improvement of Anti-CD36 Antibody Detection via Monoclonal Antibody Immobilization of Platelet Antigens Assay by Using Selected Monoclonal Antibodies. *Ann Lab Med*. 2023;43(1):86-91.

23. Xia W, Xu X, Fu Y, et al. CD36 deficiency among South-East Asian populations. *ISBT Science Series*. 2016;11(S2):33-36.

24. He H, Tang L, Jin Y, et al. High-Throughput CD36 Phenotyping on Human Platelets Based on Sandwich ELISA and Mutant Gene Analysis. *Transfus Med Hemother*. 2024;51(1):32-40.

25. Flesch BK, Scherer V, Opitz A, et al. Platelet CD36 deficiency is present in 2.6% of Arabian individuals and can cause NAIT and platelet refractoriness. *Transfusion*. 2021;61(6):1932-1942.

26. Lee K, Godeau B, Fromont P, et al. CD36 deficiency is frequent and can cause platelet immunization in Africans. *Transfusion*. 1999;39(8):873-879.

27. Curtis BR, Aster RH. Incidence of the Nak(a)-negative platelet phenotype in African Americans is similar to that of Asians. *Transfusion*. 1996;36(4):331-334.

28. Flesch B, Miller J, Repp R, et al. Successful autologous hematopoietic progenitor cell transplantation in a patient with an isoantibody against CD36 (glycoprotein IV, Naka). *Bone Marrow Transplant*. 2008;42(7):489-491.

29. Porcelijn L, Huiskes E, de Haas M. Progress and development of platelet antibody detection. *Transfusion and Apheresis Science*. 2020;59(1):102705.

30. Shin-Yi Tsai, et al. How CD36 Deficiency Intersects with Complex Diseases and Confounds Transfusion and Cardiometabolic Care: Three Cases Illustrating Diagnostic Challenges. Presented at : Blood 2025 and the 36th Regional Congress of the ISBT; 2025 Oct 26 - 29; Perth, Australia. Abstract 758.

31. Shin-Yi Tsai, Hsiao-Lin Chang, Yung-Shiu Chan, Ching-Hsiang Yu, Chen-Yu Jiang, Lin. M-L. A Case of Platelet Transfusion Refractoriness in a CD36-Deficiency Patient With Drug-Induced Thrombocytopenia. *Transfusion*. 2024;64(S3):157A.

32. Shin-Yi Tsai, et al. Diagnostic challenges and clinical impacts of CD36 deficiency in patients with multiple comorbidities: insights from two illustrative

cases. Presented at : Blood 2025 and the 36th Regional Congress of the ISBT; 2025 Oct 26 - 29; Perth, Australia. Abstract 517.

33. Lee B-C, Lin K-H, Hu C-Y, Lo S-C. Thromboelastography characterized CD36 null subjects as slow clot formation and indicative of hypocoagulability. *Thrombosis Research*. 2019;178:79-84.

34. Iba T, Levy JH, Maier CL, et al. Updated definition and scoring of disseminated intravascular coagulation in 2025: communication from the ISTH SSC Subcommittee on Disseminated Intravascular Coagulation. *Journal of Thrombosis and Haemostasis*. 2025;23(7):2356-2362.

35. Marini I, Uzun G, Jamal K, Bakchoul T. Treatment of drug-induced immune thrombocytopenias. *Haematologica*. 2022;107(6):1264-1277.

36. George JN, Aster RH. Drug-induced thrombocytopenia: pathogenesis, evaluation, and management. *Hematology Am Soc Hematol Educ Program*. 2009:153-158.

37. Sahai T, Masel D, Henrichs KF, et al. Platelet Refractoriness Due to Anti-CD-36(NAKa) Ameliorated By Platelet Washing. *Blood*. 2016;128(22):3857-3857.

38. Seftel MD, Growe GH, Petraszko T, et al. Universal prestorage leukoreduction in Canada decreases platelet alloimmunization and refractoriness. *Blood*. 2004;103(1):333-339.

39. Hawkins J, Aster RH, Curtis BR. Post-Transfusion Purpura: Current Perspectives. *J Blood Med*. 2019;10:405-415.

40. Hirunwidchayarat P, Raslan IA, Khandelwal A, Lee WL. Post-transfusion purpura in a 36-year-old woman. *Cmaj*. 2025;197(23):E640-e644.

41. Cimo PL, Aster RH. Post-transfusion purpura: successful treatment by exchange transfusion. *The New England journal of medicine*. 1972;287(6):290-292.

42. Bakchoul T, Marini I. Drug-associated thrombocytopenia. *Hematology*. 2018;2018(1):576-583.

43. Nguyen VD, Tourigny JF, Roy R, Brouillette D. Rapid-Onset Thrombocytopenia Following Piperacillin-Tazobactam Reexposure. *Pharmacotherapy*. 2015;35(12):e326-330.

44. Lieberman L, Greinacher A, Murphy MF, et al. Fetal-Neonatal Alloimmune Thrombocytopenia (FNAIT): Guidance to Reduce the Risk of Intracranial Bleeding. *Blood*. 2018;132(Supplement 1):4717-4717.

45. Lieberman L, Greinacher A, Murphy MF, et al. Fetal and neonatal alloimmune thrombocytopenia: recommendations for evidence-based practice, an international approach. *British Journal of Haematology*. 2019;185(3):549-562.

46. Billion E, Ghattas S, Jarreau PH, et al. Lowering platelet-count threshold for transfusion in preterm neonates decreases the number of transfusions without increasing severe hemorrhage events. *Eur J Pediatr*. 2024;183(10):4417-4424.

47. Winkelhorst D, Oepkes D, Lopriore E. Fetal and neonatal alloimmune thrombocytopenia: evidence based antenatal and postnatal management strategies. *Expert Rev Hematol*. 2017;10(8):729-737.

48. Ni H, Chen P, Spring CM, et al. A novel murine model of fetal and neonatal alloimmune thrombocytopenia: response to intravenous IgG therapy. *Blood*. 2006;107(7):2976-2983.

49. Winkelhorst D, Murphy MF, Greinacher A, et al. Antenatal management in fetal and neonatal alloimmune thrombocytopenia: a systematic review. *Blood*. 2017;129(11):1538-1547.

50. Murphy MF, Bussel JB. Advances in the management of alloimmune thrombocytopenia. *Br J Haematol*. 2007;136(3):366-378.

51. Lieberman L, Greinacher A, Murphy MF, et al. Fetal and neonatal alloimmune thrombocytopenia: recommendations for evidence-based practice, an international approach. *Br J Haematol*. 2019;185(3):549-562.

52. Glatz JFC, Heather LC, Luiken JJFP. CD36 as a gatekeeper of myocardial lipid metabolism and therapeutic target for metabolic disease. *Physiol Rev*. 2024;104(2):727-764.

53. Ashaq MS, Zhang S, Xu M, Li Y, Zhao B. The regulatory role of CD36 in hematopoiesis beyond fatty acid uptake. *Life Sciences*. 2024;339:122442.

54. Moon JS, Karunakaran U, Suma E, Chung SM, Won KC. The Role of CD36 in Type 2 Diabetes Mellitus: β-Cell Dysfunction and Beyond. *Diabetes Metab J*. 2020;44(2):222-233.

55. Bonstein L, Lauterbach R, Haddad N. High Incidence of Alloimmunization to Platelets and Platelet Transfusion Refractoriness during Induction Therapy in Patients Diagnosed with Acute Myeloid Leukemia. *Blood*. 2015;126(23):3484-3484.

56. Coletti K, Devine M, Ajiboye S, et al. Standardized Prophylactic Platelet Transfusion Dose for Infants Decreases Platelet Exposure without Increasing Bleeding or Transfusion Frequency. *Blood*. 2024;144:1268.

57. Metcalf RA, Nahirniak S, Guyatt G, et al. Platelet Transfusion: 2025 AABB and ICTMG International Clinical Practice Guidelines. *JAMA*. 2025;334(7):606-617.

58. Ratnasingam S, Walker PA, Tran H, et al. Bortezomib-based antibody depletion for refractory autoimmune hematological diseases. *Blood Advances*. 2016;1(1):31-35.

59. Cohn CS. Platelet transfusion refractoriness: how do I diagnose and manage? *Hematology*. 2020;2020(1):527-532.

60. Rattigan KM, Zarou MM, Helgason GV. Metabolism in stem cell–driven leukemia: parallels between hematopoiesis and immunity. *Blood*. 2023;141(21):2553-2565.

61. Yue N, Jin Q, Li C, Zhang L, Cao J, Wu C. CD36: a promising therapeutic target in hematologic tumors. *Leuk Lymphoma*. 2024;65(12):1749-1765.

62. Amantéa MC, da Silva RP, Soares LR, Pereira JLM, de Souza APD. CD36 as a marker of acute myeloid leukemia prognosis: A systematic review. *Hematol Transfus Cell Ther*. 2025;47(3):103861.

63. Love-Gregory L, Sherva R, Schappe T, et al. Common CD36 SNPs reduce protein expression and may contribute to a protective atherogenic profile. *Hum Mol Genet*. 2011;20(1):193-201.

64. Bendas G, Schlesinger M. The Role of CD36/GPIV in Platelet Biology. *Semin Thromb Hemost*. 2024;50(2):224-235.

65. Zhao L, Varghese Z, Moorhead JF, Chen Y, Ruan XZ. CD36 and lipid metabolism in the evolution of atherosclerosis. *British Medical Bulletin*. 2018;126(1):101-112.

66. Favaloro EJ, Pasalic L, Lippi G. Editorial Compilation XIV. *Semin Thromb Hemost*. 2023;50(02):151-156.

67. Tian K, Xu Y, Sahebkar A, Xu S. CD36 in Atherosclerosis: Pathophysiological Mechanisms and Therapeutic Implications. *Curr Atheroscler Rep*. 2020;22(10):59.

68. Shu H, Peng Y, Hang W, Nie J, Zhou N. The Role of CD36 in Cardiovascular Disease: A Critical Review; 2024:49-84.

69. Fujita S, Terasaki F, Morishima I, Hoshiga M. Cardiomyopathy Associated with CD36 Deficiency: Role of (18)F-Fluorodeoxyglucose Positron Emission Tomography in the Diagnosis. *Intern Med*. 2024;63(22):3059-3064.

70. Tsubokawa T, Nakamura M, Miyazaki E, et al. Perioperative Management of a Patient With CD36 Deficiency Undergoing Urgent Cardiac Surgery. *Journal of Cardiothoracic and Vascular Anesthesia*. 2022;36(8):3149-3151.

71. Glatz JFC, Heather LC, Luiken JJFP. CD36 as a gatekeeper of myocardial lipid metabolism and therapeutic target for metabolic disease. *Physiological Reviews*. 2023;104(2):727-764.

72. Li W, Febbraio M, Reddy SP, Yu D-Y, Yamamoto M, Silverstein RL. CD36 participates in a signaling pathway that regulates ROS formation in murine VSMCs. *The Journal of Clinical Investigation*. 2010;120(11):3996-4006.

73. Kim E-H, Tolhurst AT, Szeto HH, Cho S-H. Targeting CD36-Mediated Inflammation Reduces Acute Brain Injury in Transient, but not Permanent, Ischemic Stroke. *CNS Neuroscience & Therapeutics*. 2015;21(4):385-391.

74. Balkaya M, Kim ID, Shakil F, Cho S. CD36 deficiency reduces chronic BBB dysfunction and scar formation and improves activity, hedonic and memory deficits in ischemic stroke. *J Cereb Blood Flow Metab*. 2021;41(3):486-501.

75. Pedini P, Hicheri Y, Bertand G, et al. A case of platelet transfusion refractoriness in a CD36-negative patient with acute myeloid leukemia: Diagnostic and therapeutic management. *Transfusion*. 2022;62:2148-2150.

76. Chen Y, Zhang J, Cui W, Silverstein RL. CD36, a signaling receptor and fatty acid transporter that regulates immune cell metabolism and fate. *Journal of Experimental Medicine*. 2022;219(6):e20211314.

77. Jiang M, Karsenberg R, Bianchi F, van den Bogaart G. CD36 as a double-edged sword in cancer. *Immunology Letters*. 2024;265:7-15.

78. Olonisakin TF, Li H, Xiong Z, et al. CD36 Provides Host Protection Against Klebsiella pneumoniae Intrapulmonary Infection by Enhancing

Lipopolysaccharide Responsiveness and Macrophage Phagocytosis. *The Journal of Infectious Diseases*. 2016;214(12):1865-1875.

79. Baranova IN, Kurlander R, Bocharov AV, et al. Role of human CD36 in bacterial recognition, phagocytosis, and pathogen-induced JNK-mediated signaling. *J Immunol*. 2008;181(10):7147-7156.

80. Salama OS, Aladl DA, El Ghannam DM, Elderiny WE. Evaluation of platelet cross-matching in the management of patients refractory to platelet transfusions. *Blood Transfus*. 2014;12(2):187-194.

81. Liu Y, Zhang Y, Chen D, Fu Y. Current Status of and Global Trends in Platelet Transfusion Refractoriness From 2004 to 2021: A Bibliometric Analysis. *Front Med (Lausanne)*. 2022;9:873500.

82. Slichter SJ, Fish D, Abrams VK, Gaur L, Nelson K, Bolgiano D. Evaluation of different methods of leukoreduction of donor platelets to prevent alloimmune platelet refractoriness and induce tolerance in a canine transfusion model. *Blood*. 2005;105(2):847-854.

83. van Osch TLJ, Oosterhoff JJ, Bentlage AEH, et al. Fc galactosylation of anti-platelet human IgG1 alloantibodies enhances complement activation on platelets. *Haematologica*. 2022;107(10):2432-2444.

84. Usmani SZ, Weiss BM, Plesner T, et al. Clinical efficacy of daratumumab monotherapy in patients with heavily pretreated relapsed or refractory multiple myeloma. *Blood*. 2016;128(1):37-44.

85. Khatri SS, Curtis BR, Yamada C. A case of platelet transfusion refractoriness due to anti-CD36 with a successful treatment outcome. *Immunohematology*. 2019;35(4):139-144.

Figure Legend

Figure 1. Clinical timeline and therapeutic interventions. The figure delineates the sequential clinical interventions, highlighting the initiation and progression of large-volume blood transfusion therapy, hemodialysis (H/D), and plasma exchange (PE). Each intervention point corresponds precisely with the patient's clinical deterioration and therapeutic escalation during hospitalization. A comprehensive summary of the above interventions and corresponding renal functions (the level of creatinine, BUN) and liver functions (the level of total and direct bilirubin) dynamics was depicted and recorded by dates in the patient's hospitalization.

Figure 2. Comprehensive Timeline of Antibiotic Therapy, Transfusion Interventions, and Hemostatic Dynamics During Hospitalization. (A) A comprehensive summary of antibiotic interventions and corresponding platelet

dynamics is depicted and recorded by patient hospitalization dates. **(B)** Transfusion timeline and platelet response during hospitalization. A comprehensive summary of transfusion interventions and corresponding platelet dynamics is depicted, including administration of 44 units of packed red blood cells, 32 apheresis platelet units of which four were specifically CD36-negative, 30 units of fresh frozen plasma, 28 designated for plasma exchange procedures, and six units of frozen plasma, and 1 unit of whole blood. Serial platelet counts are illustrated before and after platelet transfusions, with blood sampling intervals indicated. This figure highlights the temporal relationship between transfusion strategies, particularly CD36-negative platelet transfusions, and the patient's count response amidst ongoing immune-mediated platelet refractoriness and concomitant clinical complexities. **(C)** The corresponding levels of coagulopathy, relevant lab data, such as PT/APTT/INR, hemoglobin, and platelet dynamics, are depicted and recorded by the patient's hospitalization dates.

Figure 3. Detection of anti-CD36 antibody in sera by flow cytometric analysis. (A) Overlay histograms compare patient serum (purple), CD36(-) control, and CD36(+) control. The patient's curve aligns closely with the CD36(-) control, showing a sharp peak at low fluorescence (FITC-A), with minimal rightward shift. The CD36(+) control demonstrates an apparent change to higher fluorescence, confirming strong CD36 antigen expression. The absence of a comparable rightward change in the patient

sample indicates a lack of anti-CD36 antibody binding, consistent with CD36 deficiency. **(B)** Separated histograms clearly show the distribution for each population: patient, CD36(-) control, and CD36(+) control. The patient and CD36(-) control overlap extensively, reinforcing the finding that the patient's platelets do not express CD36 and do not bind anti-CD36 antibody. The CD36(+) control shows a distinct peak at higher fluorescence, as expected for CD36-expressing cells. **(C)** PerCP-Cy5.5-A histogram overlays patient (blue), CD36(-) control, and CD36(+) control. The patient's and CD36(-) control's histograms peak at low fluorescence, with no detectable population at higher intensity, while the CD36(+) control displays a broad peak in the high-intensity range. This confirms the absence of CD36 on the patient's platelets, validating the CD36-deficient phenotype both by negative immunoreactivity and by comparison to well-characterized controls.

Summary interpretation: These histograms collectively demonstrate that the patient's platelets lack CD36 antigen expression, as their fluorescence profiles are indistinguishable from CD36(-) controls and distinct from CD36(+) controls. This pattern is diagnostic for type I or type II CD36 deficiency and supports the absence of detectable anti-CD36 antibodies in the patient's serum by flow cytometry. **(D)** Clinical manifestations of severe disseminated intravascular coagulation (DIC) in a critically ill patient. The images depict extensive, confluent ecchymoses and purpuric lesions

involving multiple anatomical sites, including bilateral axillary regions, the lateral thoracic wall, and extending along the upper extremities. The right thigh showed ruptured bullae and extensive macular ecchymoses surrounding it. These severe dermatologic involvement and widespread capillary leakage illustrate the profound hemorrhagic and thrombotic complications characteristic of PTR and advanced DIC, highlighting the clinical severity and extensive vascular compromise that may arise in such cases. All images have been carefully de-identified to maintain patient confidentiality.

Figure 4. Maternal Type I CD36 Deficiency Confirmed by Flow Cytometry. Flow cytometry showed no CD36 antigen on maternal platelets or monocytes (maternal plots with anti-CD36 overlapped isotype controls, whereas the father's platelets/monocytes (and a standard donor control) were strongly CD36-positive. This pattern indicates a maternal Type I CD36 deficiency, well-recognized in Asian populations, and predisposes to alloimmunization during pregnancy. By contrast, paternal cells express CD36 normally. In NAIT, a CD36-deficient (mother) × CD36-positive (father) pairing is a classic scenario: the mother can form anti-CD36 (Nak) antibodies against the fetal platelets.

Figure 5. Functional Assessment of Platelet and Monocyte CD36 Expression and IgM Binding Flow cytometric panels depict:

(A) CD36 expression on platelets (PSP-CD36Ab(+)-CD36). Top-left panel: Dot plot showing PerCP-conjugated Mouse Anti-Human CD41a fluorescence intensity (X-axis) versus forward scatter (cell size, Y-axis). The rectangular gate isolates the platelet population, leveraging platelet-specific CD41a expression and size characteristics to ensure accurate identification. Top-left panel: Two-parameter dot plot of FITC-conjugated Mouse Anti-Human CD36 (X-axis) versus PerCP-conjugated CD41a (Y-axis). Platelets -expressing CD41a and CD36 are depicted as red events in the upper-right quadrant, indicating a CD36-positive platelet subpopulation at 0.16% of the gated platelets. Bottom-left panel: Histogram illustrating CD36 fluorescence intensity across the gated platelet population. The mean fluorescence intensity (MFI) threshold defining CD36 positivity exceeds 10 (Log scale), consistent with established gating criteria used in quantitative assays of platelet CD36 expression. This threshold distinguishes CD36-deficient and CD36-expressing platelets, as commonly applied in clinical flow cytometry analyses.

(B) Platelet-bound IgM levels (PSP-CD36Ab(+)-IgM). Top-left panel: Dot plot showing PerCP-conjugated Mouse Anti-Human CD41a fluorescence intensity (X-axis) versus forward scatter (cell size, Y-axis). The rectangular gate isolates the platelet population, leveraging platelet-specific CD41a expression and size characteristics to ensure accurate identification. Top-right panel: Two-parameter dot plot of FITC-

conjugated IgM (X-axis) versus PerCP-conjugated CD41a (Y-axis). Platelets -expressing CD41a and IgM are depicted as red events in the upper-right quadrant, indicating a minimal IgM-positive platelet subpopulation at 0.06% of the gated platelets. Bottom-left panel: Histogram illustrating IgM fluorescence intensity across the gated platelet population. The mean fluorescence intensity (MFI) threshold defining IgM positivity exceeds 10 (Log scale), consistent with clinical gating standards. The extremely low IgM binding suggests minimal non-specific IgM interaction on the platelet surface. FITC-conjugated IgM (Isotype Control) is used to set the negative fluorescence intensity and is as the negative control

(C) CD36 expression on monocytes (WB-CD36Ab(+)-CD36). Top-left panel: Dot plot showing PerCP-conjugated Mouse Anti-Human CD14 fluorescence intensity (X-axis) versus forward scatter (cell size, Y-axis). The rectangular gate isolates the monocyte population, leveraging CD14 expression and size characteristics for accurate identification. Top-right panel: Two-parameter dot plot of FITC-conjugated Mouse Anti-Human CD36 (X-axis) versus PerCP-conjugated CD14 (Y-axis). In the upper right quadrant, Monocytes co-expressing CD14 and CD36 are depicted as red events, indicating a CD36-positive monocyte subpopulation at 1.30% of the gated monocytes. Bottom-left panel: Histogram illustrating CD36 fluorescence intensity across the gated monocyte population. The mean fluorescence intensity (MFI) threshold defining CD36

positivity exceeds 100 (Log scale), consistent with established gating criteria. This enables accurate differentiation between CD36-deficient and CD36-expressing monocytes.

(D) Monocyte-bound IgM levels (WB-CD36Ab(+)-IgM). Top-left panel: Dot plot showing PerCP-conjugated Mouse Anti-Human CD14 fluorescence intensity (X-axis) versus forward scatter (cell size, Y-axis). The rectangular gate isolates the monocyte population, leveraging CD14 expression and size characteristics for accurate identification. Top-right panel: Two-parameter dot plot of FITC-conjugated IgM (X-axis) versus PerCP-conjugated CD14 (Y-axis). In the upper right quadrant, Monocytes co-expressing CD14 and IgM are depicted as red events, indicating a small IgM-positive monocyte subpopulation at 0.92% of the gated monocytes. Bottom-left panel: Histogram illustrating IgM fluorescence intensity across the gated monocyte population. The MFI threshold defining IgM positivity exceeds 10 (Log scale), which aligns with clinical flow cytometry gating standards. The low positivity rate indicates minimal IgM surface binding. FITC-conjugated IgM (Isotype Control) is used to set the negative fluorescence intensity and is as the negative control.

(E) Molecular Characterization of CD36 Deficiency: Identification of Pathogenic Variants by Sanger Sequencing. This figure illustrates representative gene sequencing chromatograms from patients diagnosed with type I CD36 deficiency,

highlighting distinct pathogenic variants across exon 5 of the CD36 gene. The panel displays a 2-base pair deletion (c. 329_330delAC) (rs572295823) in exon 5, observed in a homozygous state.

Figure 6. Validation of CD36 Deficiency and Alloimmunization Mechanisms

Flow cytometric analysis demonstrates:

(A) Platelet CD36 expression (PSP-M2(D1)-CD36). Top-left panel: Dot plot showing PerCP-conjugated Mouse Anti-Human CD41a fluorescence intensity (X-axis) versus forward scatter (cell size, Y-axis). The rectangular gate isolates the platelet population, leveraging platelet-specific CD41a expression and size characteristics to ensure accurate identification. Top-right panel: Two-parameter dot plot of FITC-conjugated Mouse Anti-Human CD36 (X-axis) versus PerCP-conjugated CD41a (Y-axis). Platelets -expressing CD41a and CD36 are depicted as red events in the upper-right quadrant, indicating a CD36-positive platelet subpopulation at 1.89% of the gated platelets. Bottom-left panel: Histogram illustrating CD36 fluorescence intensity across the gated platelet population. The mean fluorescence intensity (MFI) threshold defining CD36 positivity exceeds 10 (Log scale), consistent with established gating criteria used in quantitative assays of platelet CD36 expression. This threshold distinguishes CD36-deficient and CD36-expressing platelets, as commonly applied in clinical flow cytometry analyses.

(B) Platelet IgM binding (PSP-M2(D1)-IgM). Top-left panel: Dot plot showing PerCP-conjugated Mouse Anti-Human CD41a fluorescence intensity (X-axis) versus forward scatter (cell size, Y-axis). The rectangular gate isolates the platelet population, leveraging platelet-specific CD41a expression and size characteristics to ensure accurate identification. Top-right panel: Two-parameter dot plot of FITC-conjugated IgM (X-axis) versus PerCP-conjugated CD41a (Y-axis). Platelets -expressing CD41a and IgM are depicted as red events in the upper-right quadrant, indicating a minimal IgM-positive platelet subpopulation at 0.04% of the gated platelets. Bottom-left panel: Histogram illustrating IgM fluorescence intensity across the gated platelet population. The MFI threshold defining IgM positivity exceeds 10 (Log scale), which aligns with accepted gating standards. The low positive event count supports this sample's rarity of IgM surface binding. FITC-conjugated IgM (Isotype Control) is used to set the negative fluorescence intensity and is as the negative control.

(C) Monocyte CD36 expression (WB-M2(D1)-CD36). Top-left panel: Dot plot showing PerCP-conjugated Mouse Anti-Human CD14 fluorescence intensity (X-axis) versus forward scatter (cell size, Y-axis). The rectangular gate isolates the monocyte population, leveraging CD14 expression and size characteristics for accurate identification. Top-right panel: Two-parameter dot plot of FITC-conjugated Mouse Anti-Human CD36 (X-axis) versus PerCP-conjugated CD14 (Y-axis). In the upper

right quadrant, Monocytes co-expressing CD14 and CD36 are depicted as red events, indicating a CD36-positive monocyte subpopulation at 1.54% of the gated monocytes. Bottom-left panel: Histogram illustrating CD36 fluorescence intensity across the gated monocyte population. The MFI threshold defining CD36 positivity exceeds 100 (Log scale), enabling the differentiation of CD36-deficient from CD36-expressing monocytes, consistent with clinical flow cytometry gating standards.

(D) Monocyte IgM binding (WB-M2(D1)-IgM). Top-left panel: Dot plot showing PerCP-conjugated Mouse Anti-Human CD14 fluorescence intensity (X-axis) versus forward scatter (cell size, Y-axis). The rectangular gate isolates the monocyte population, leveraging CD14 expression and size characteristics for accurate identification. Top-right panel: Two-parameter dot plot of FITC-conjugated IgM (X-axis) versus PerCP-conjugated CD14 (Y-axis). Monocytes co-expressing CD14 and IgM are depicted as red events in the upper-right quadrant, indicating a small IgM-positive monocyte subpopulation at 0.70% of the gated monocytes. Bottom-left panel: Histogram illustrating IgM fluorescence intensity across the gated monocyte population. The MFI threshold defining IgM positivity exceeds 10 (Log scale), consistent with established clinical flow cytometry gating criteria. The low positive percentage suggests minimal IgM surface binding. FITC-conjugated IgM (Isotype Control) is used to set the negative fluorescence intensity and is as the negative control.

(E) Molecular Characterization of CD36 Deficiency: Identification of Pathogenic Variants by Sanger Sequencing. This figure illustrates representative gene sequencing chromatograms from patients diagnosed with type I CD36 deficiency, highlighting distinct pathogenic variants across exon 5 of the CD36 gene. The panel presents a frameshift mutation (c.329_330delAC) (rs572295823)in exon 5, introducing a premature shift in the reading frame at amino acid 110, predicted to generate a truncated, non-functional protein.

Figure 7. Flow Cytometric Confirmation of Type I CD36 Deficiency and Anti-CD36 Alloantibody Detection Shows absence of CD36 expression on patient platelets and monocytes, coupled with specific anti-CD36 IgG binding on CD36-positive targets, confirming type I CD36 deficiency and alloimmunization.

(A-C) Flow cytometric analysis of CD36 antigen expression on patient blood cells. Peripheral blood samples were analyzed using PerCP-Cy5.5–conjugated goat anti-human CD36 antibody and matched isotype controls. Flow cytometry shows absent CD36 expression on both platelets and monocytes, confirmed using PerCP-Cy5.5–conjugated anti-CD36 antibody and matched isotype controls. Positive control monocytes from a healthy donor validate assay specificity.

(D-F) Patient and control sera were incubated separately with CD36-negative and CD36-positive platelet targets, followed by FITC-conjugated goat anti-human IgG. **(D)**

Patient serum + CD36– platelets: Histogram overlay of FITC fluorescence for CD36– platelets incubated with patient serum (blue) versus negative control serum (purple) shows only background binding. **(E) Patient serum + CD36+ platelets:** Corresponding overlay for CD36+ platelets revealed a marked rightward shift with patient serum (red), indicating specific anti-CD36 IgG binding; negative control serum (purple) remains at background. **(F) Positive control serum + CD36+ platelets:** FITC fluorescence of CD36+ platelets incubated with patient serum (pink) exhibits a similar rightward shift relative to negative control (purple), confirming assay sensitivity and specificity.

(G-H) Platelet Immunofluorescence Assay (PIFA) Confirms Anti-CD36 Antibody Binding. Immunofluorescence images demonstrate specific binding of anti-CD36 antibodies from patient and positive control sera to CD36-positive platelets, with no reactivity on CD36-negative targets, validating assay specificity. **(I-J)** Differential CD36 Expression in Platelets and Monocytes by Flow Cytometry. The panels demonstrate absent CD36 expression on both patient platelets and monocytes. These findings are consistent with a **CD36-deficiency type I** phenotype.

Figures

Figure 1

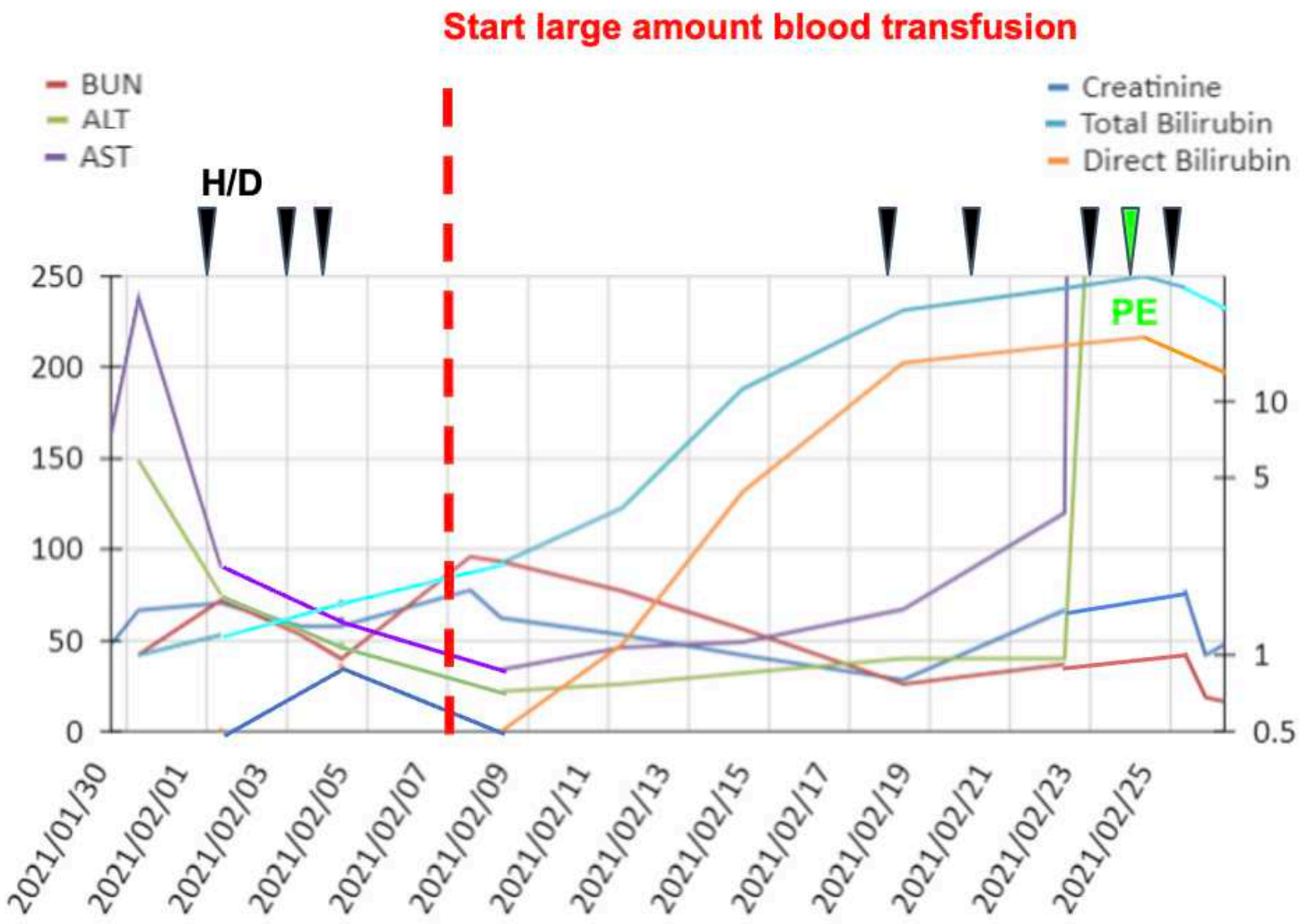

Figure 1

Clinical timeline and therapeutic interventions. The figure delineates the sequential clinical interventions, highlighting the initiation and progression of large-volume blood transfusion therapy, hemodialysis (H/D), and plasma exchange (PE). Each intervention point corresponds precisely with the patient's clinical deterioration and therapeutic escalation during hospitalization. A comprehensive summary of the above interventions and corresponding renal functions (the level of creatinine, BUN) and liver functions (the level of total and direct bilirubin) dynamics was depicted and recorded by dates in the patient's hospitalization.

Figure 2

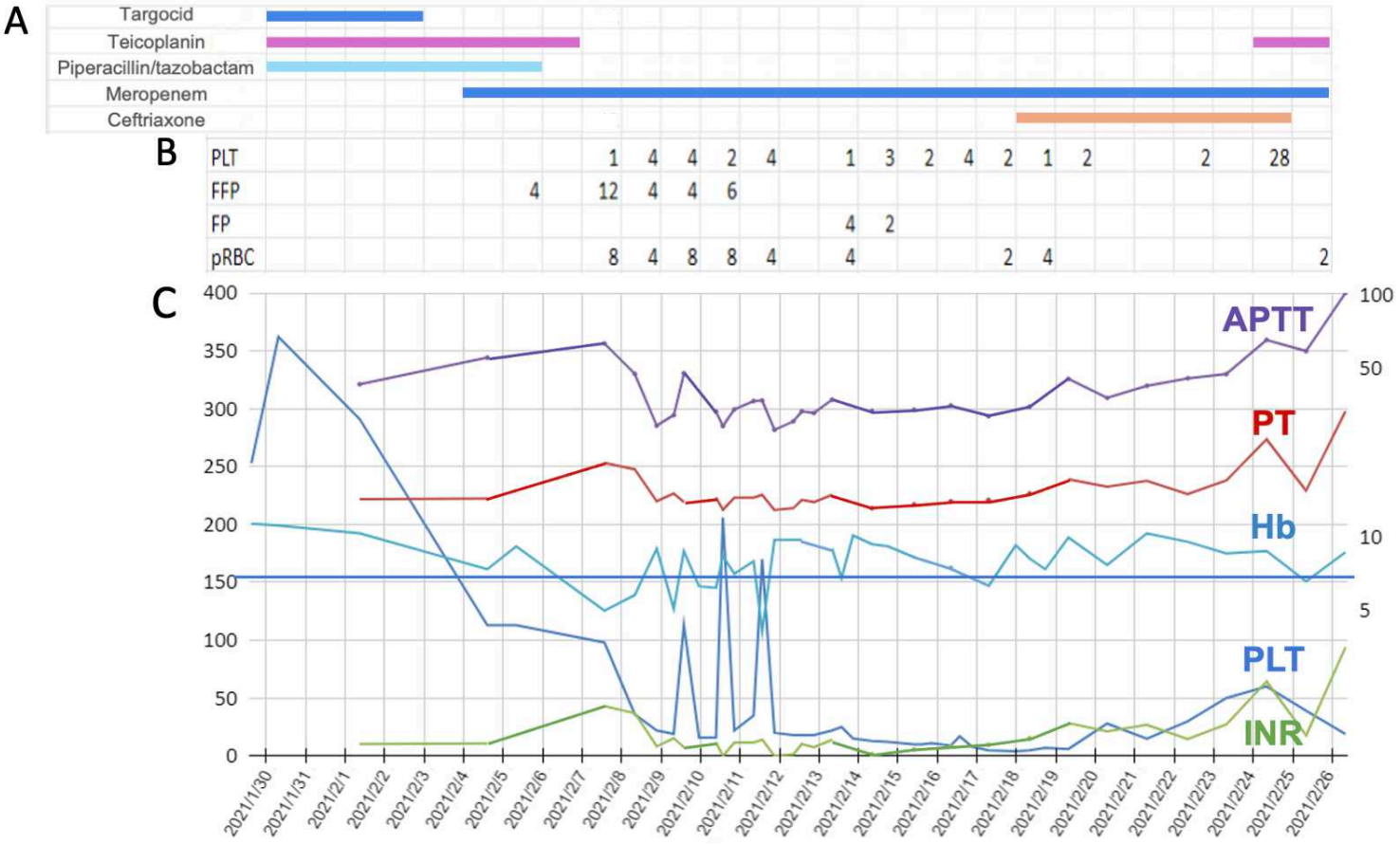

Figure 2

Comprehensive Timeline of Antibiotic Therapy, Transfusion Interventions, and Hemostatic Dynamics During Hospitalization. (A) A comprehensive summary of antibiotic interventions and corresponding platelet dynamics is depicted and recorded by patient hospitalization dates. **(B)** Transfusion timeline and platelet response during hospitalization. A comprehensive summary of transfusion interventions and corresponding platelet dynamics is depicted, including administration of 44 units of packed red blood cells, 32 apheresis platelet units of which four were specifically CD36-negative, 30 units of fresh frozen plasma, 28 designated for plasma exchange procedures, and six units of frozen plasma, and 1 unit of whole blood. Serial platelet counts are illustrated before and after platelet transfusions, with blood sampling intervals indicated. This figure highlights the temporal relationship between transfusion strategies, particularly CD36-negative platelet transfusions, and the patient's count response amidst ongoing immune-mediated platelet refractoriness and concomitant clinical complexities. **(C)** The corresponding levels of coagulopathy, relevant lab data, such as PT/APTT/INR, hemoglobin, and platelet dynamics, are depicted and recorded by the patient's hospitalization dates.

Figure 3

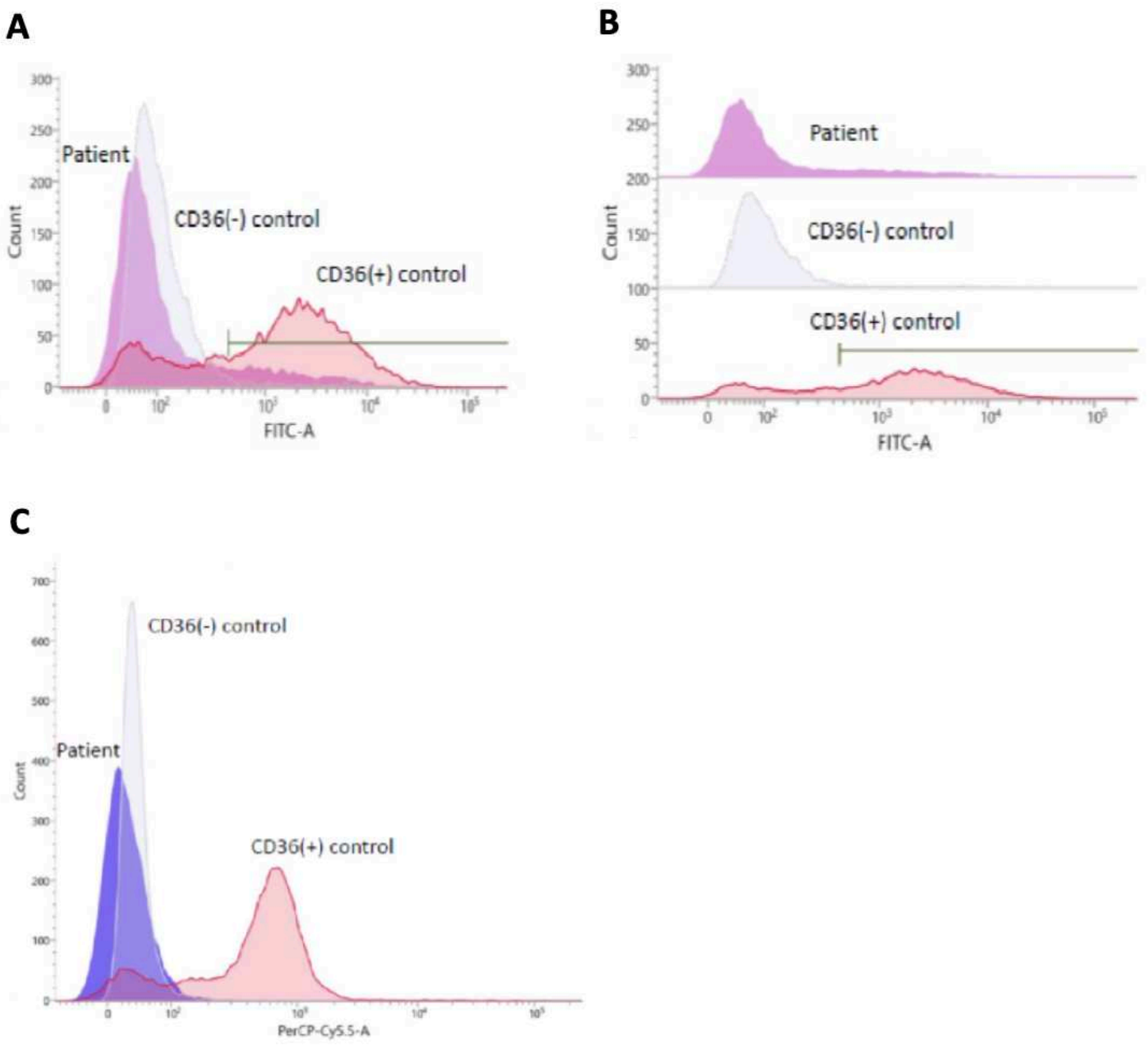

Figure 3

Detection of anti-CD36 antibody in sera by flow cytometric analysis. (A) Overlay histograms compare patient serum (purple), CD36(-) control, and CD36(+) control. The patient's curve aligns closely with the CD36(-) control, showing a sharp peak at low fluorescence (FITC-A), with minimal rightward shift. The CD36(+) control demonstrates an apparent change to higher fluorescence, confirming strong CD36 antigen expression. The absence of a comparable rightward change in the patient sample indicates a lack of anti-CD36 antibody binding, consistent with CD36 deficiency. **(B)** Separated histograms clearly

show the distribution for each population: patient, CD36(-) control, and CD36(+) control. The patient and CD36(-) control overlap extensively, reinforcing the finding that the patient's platelets do not express CD36 and do not bind anti-CD36 antibody. The CD36(+) control shows a distinct peak at higher fluorescence, as expected for CD36-expressing cells. **(C)** PerCP-Cy5.5-A histogram overlays patient (blue), CD36(-) control, and CD36(+) control. The patient's and CD36(-) control's histograms peak at low fluorescence, with no detectable population at higher intensity, while the CD36(+) control displays a broad peak in the high-intensity range. This confirms the absence of CD36 on the patient's platelets, validating the CD36-deficient phenotype both by negative immunoreactivity and by comparison to well-characterized controls.

Summary interpretation: These histograms collectively demonstrate that the patient's platelets lack CD36 antigen expression, as their fluorescence profiles are indistinguishable from CD36(-) controls and distinct from CD36(+) controls. This pattern is diagnostic for type I or type II CD36 deficiency and supports the absence of detectable anti-CD36 antibodies in the patient's serum by flow cytometry. **(D)**Clinical manifestations of severe disseminated intravascular coagulation (DIC) in a critically ill patient. The images depict extensive, confluent ecchymoses and purpuric lesions involving multiple anatomical sites, including bilateral axillary regions, the lateral thoracic wall, and extending along the upper extremities. The right thigh showed ruptured bullae and extensive macular ecchymoses surrounding it. These severe dermatologic involvement and widespread capillary leakage illustrate the profound hemorrhagic and thrombotic complications characteristic of PTR and advanced DIC, highlighting the clinical severity and extensive vascular compromise that may arise in such cases. All images have been carefully de-identified to maintain patient confidentiality.

Figure 4

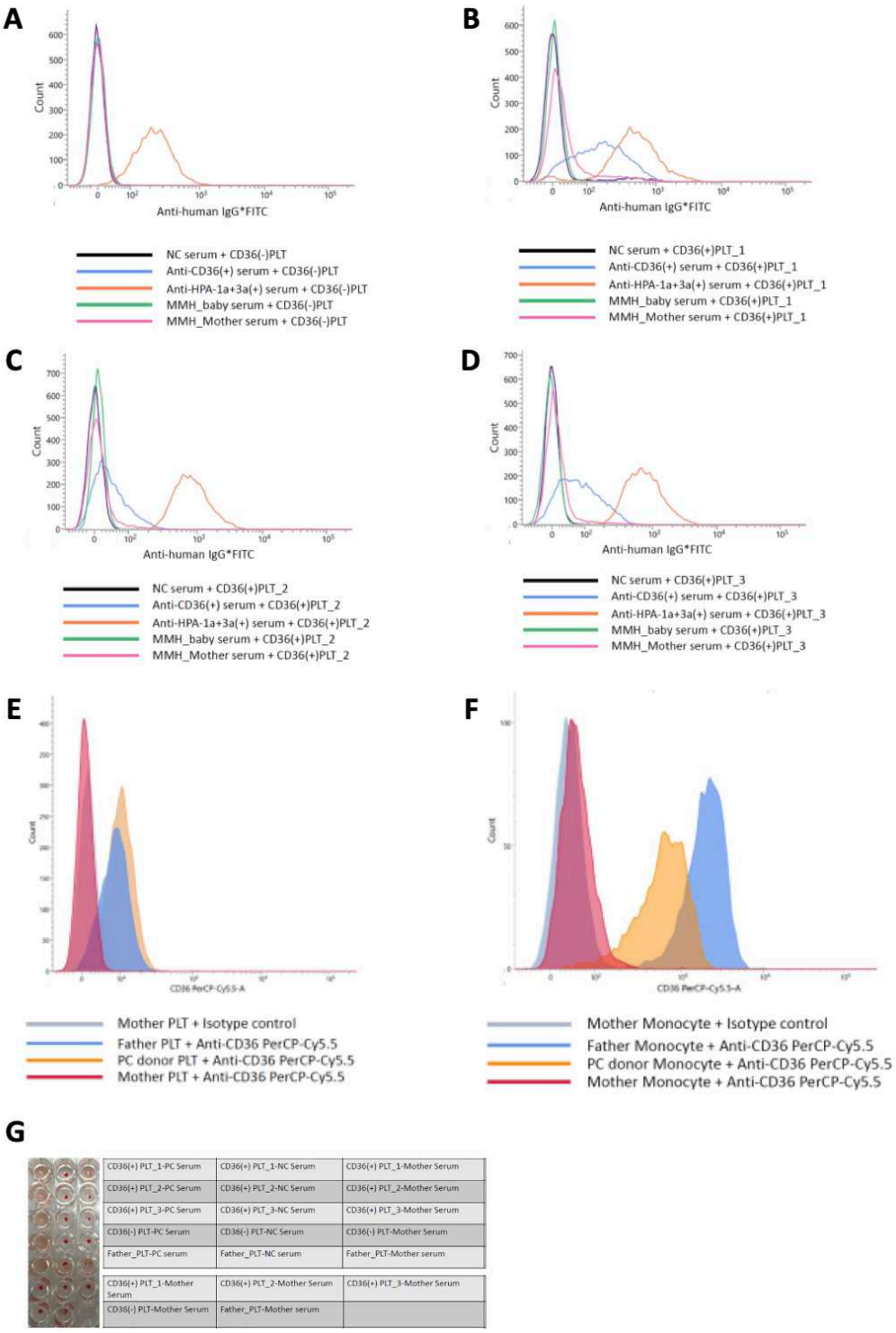

Figure 4

Maternal Type I CD36 Deficiency Confirmed by Flow Cytometry. Flow cytometry showed no CD36 antigen on maternal platelets or monocytes (maternal plots with anti-CD36 overlapped isotype controls, whereas the father's platelets/monocytes (and a standard donor control) were strongly CD36-positive. This pattern indicates a maternal Type I CD36 deficiency, well-recognized in Asian populations, and predisposes to alloimmunization during pregnancy. By contrast, paternal cells express CD36 normally. In

NAIT, a CD36-deficient (mother) × CD36-positive (father) pairing is a classic scenario: the mother can form anti-CD36 (Nak) antibodies against the fetal platelets.

Figure 5

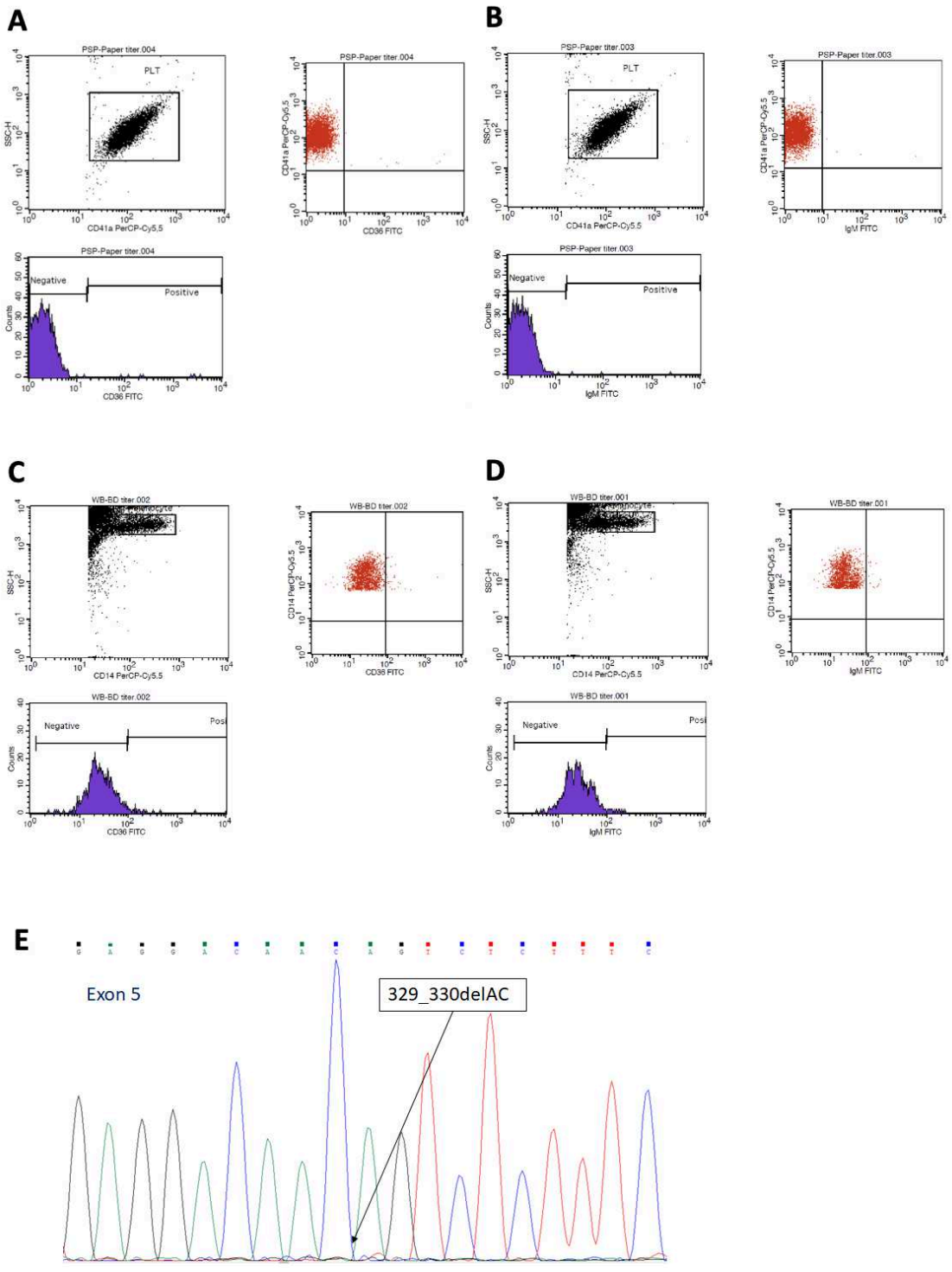

Figure 5

Functional Assessment of Platelet and Monocyte CD36 Expression and IgM Binding Flow cytometric panels depict:

(A) CD36 expression on platelets (PSP-CD36Ab(+)-CD36). Top-left panel: Dot plot showing PerCP□conjugated Mouse Anti□Human CD41a fluorescence intensity (X-axis) versus forward scatter (cell size, Y-axis). The rectangular gate isolates the platelet population, leveraging platelet-specific CD41a expression and size characteristics to ensure accurate identification. Top-left panel: Two-parameter dot plot of FITC□conjugated Mouse Anti□Human CD36 (X-axis) versus PerCP□conjugated CD41a (Y-axis). Platelets □expressing CD41a and CD36 are depicted as red events in the upper□right quadrant, indicating a CD36-positive platelet subpopulation at 0.16% of the gated platelets. Bottom-left panel: Histogram illustrating CD36 fluorescence intensity across the gated platelet population. The mean fluorescence intensity (MFI) threshold defining CD36 positivity exceeds 10 (Log scale), consistent with established gating criteria used in quantitative assays of platelet CD36 expression. This threshold distinguishes CD36-deficient and CD36-expressing platelets, as commonly applied in clinical flow cytometry analyses.

(B) Platelet-bound IgM levels (PSP-CD36Ab(+)-IgM). Top-left panel: Dot plot showing PerCP□conjugated Mouse Anti□Human CD41a fluorescence intensity (X-axis) versus forward scatter (cell size, Y-axis). The rectangular gate isolates the platelet population, leveraging platelet-specific CD41a expression and size characteristics to ensure accurate identification. Top-right panel: Two-parameter dot plot of FITC-conjugated IgM (X-axis) versus PerCP-conjugated CD41a (Y-axis). Platelets □expressing CD41a and IgM are depicted as red events in the upper□right quadrant, indicating a minimal IgM-positive platelet subpopulation at 0.06% of the gated platelets. Bottom-left panel: Histogram illustrating IgM fluorescence intensity across the gated platelet population. The mean fluorescence intensity (MFI) threshold defining IgM positivity exceeds 10 (Log scale), consistent with clinical gating standards. The extremely low IgM binding suggests minimal non-specific IgM interaction on the platelet surface. FITC-conjugated IgM (Isotype Control) is used to set the negative fluorescence intensity and is as the negative control

(C) CD36 expression on monocytes (WB-CD36Ab(+)-CD36). Top-left panel: Dot plot showing PerCP□conjugated Mouse Anti□Human CD14 fluorescence intensity (X-axis) versus forward scatter (cell size, Y-axis). The rectangular gate isolates the monocyte population, leveraging CD14 expression and size characteristics for accurate identification. Top-right panel: Two-parameter dot plot of FITC-conjugated Mouse Anti-Human CD36 (X-axis) versus PerCP-conjugated CD14 (Y-axis). In the upper right quadrant, Monocytes co□expressing CD14 and CD36 are depicted as red events, indicating a CD36-positive monocyte subpopulation at 1.30% of the gated monocytes. Bottom-left panel: Histogram illustrating CD36 fluorescence intensity across the gated monocyte population. The mean fluorescence intensity (MFI) threshold defining CD36 positivity exceeds 100 (Log scale), consistent with established gating criteria. This enables accurate differentiation between CD36-deficient and CD36-expressing monocytes.

(D) Monocyte-bound IgM levels (WB-CD36Ab(+)-IgM). Top-left panel: Dot plot showing PerCP□conjugated Mouse Anti□Human CD14 fluorescence intensity (X-axis) versus forward scatter (cell size, Y-axis). The rectangular gate isolates the monocyte population, leveraging CD14 expression and size characteristics for accurate identification. Top-right panel: Two-parameter dot plot of FITC-conjugated IgM (X-axis) versus PerCP-conjugated CD14 (Y-axis). In the upper right quadrant, Monocytes

co‐expressing CD14 and IgM are depicted as red events, indicating a small IgM-positive monocyte subpopulation at 0.92% of the gated monocytes. Bottom-left panel: Histogram illustrating IgM fluorescence intensity across the gated monocyte population. The MFI threshold defining IgM positivity exceeds 10 (Log scale), which aligns with clinical flow cytometry gating standards. The low positivity rate indicates minimal IgM surface binding. FITC-conjugated IgM (Isotype Control) is used to set the negative fluorescence intensity and is as the negative control.

(E) Molecular Characterization of CD36 Deficiency: Identification of Pathogenic Variants by Sanger Sequencing. This figure illustrates representative gene sequencing chromatograms from patients diagnosed with type I CD36 deficiency, highlighting distinct pathogenic variants across exon 5 of the CD36 gene. The panel displays a 2-base pair deletion (c. 329_330delAC) (rs572295823) in exon 5, observed in a homozygous state.

Figure 6

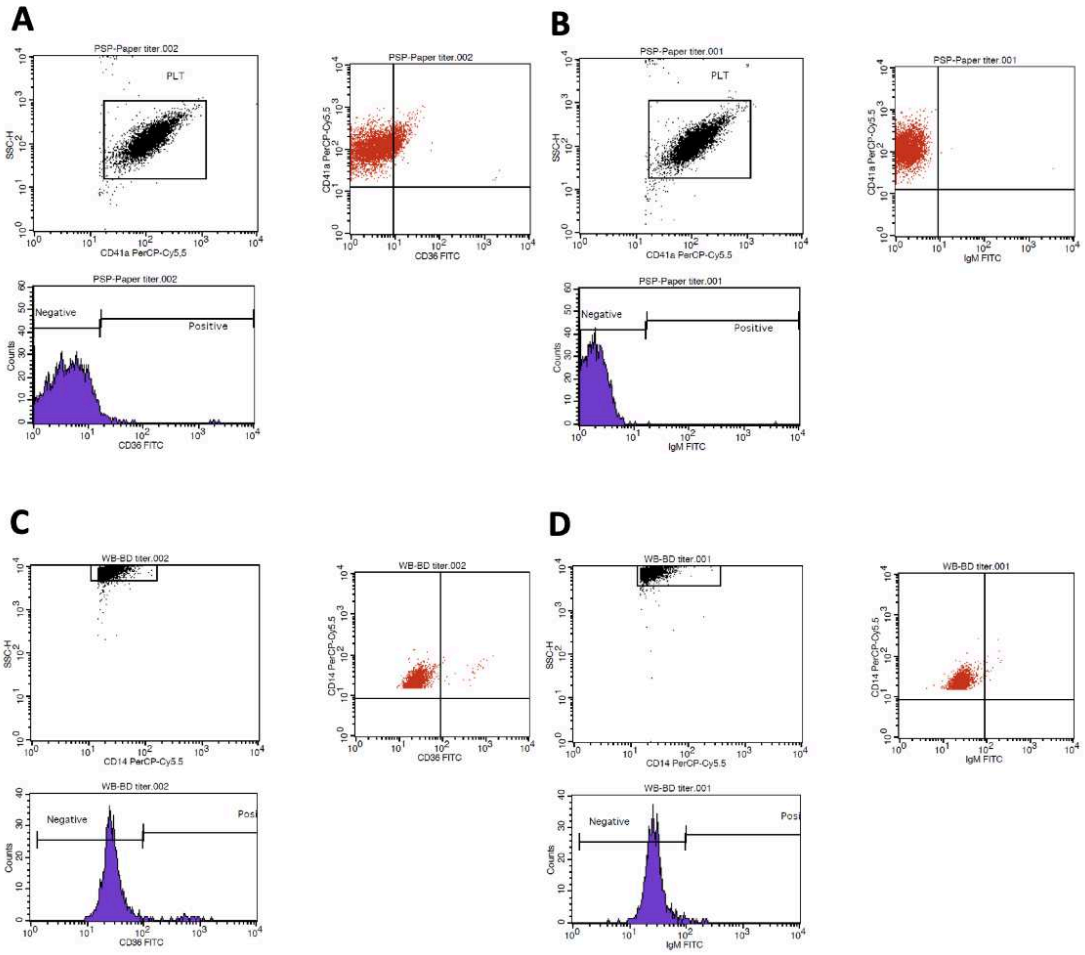

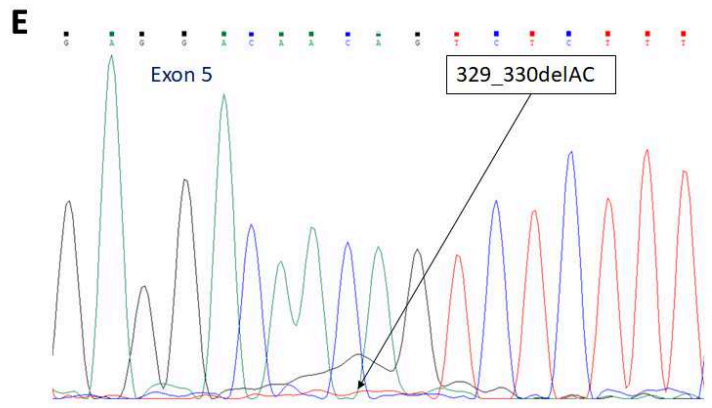

Figure 6

Validation of CD36 Deficiency and Alloimmunization Mechanisms

Flow cytometric analysis demonstrates:

(A) Platelet CD36 expression (PSP-M2(D1)-CD36). Top-left panel: Dot plot showing PerCP□conjugated Mouse Anti□Human CD41a fluorescence intensity (X-axis) versus forward scatter (cell size, Y-axis). The rectangular gate isolates the platelet population, leveraging platelet-specific CD41a expression and size characteristics to ensure accurate identification. Top-right panel: Two-parameter dot plot of FITC-conjugated Mouse Anti-Human CD36 (X-axis) versus PerCP-conjugated CD41a (Y-axis). Platelets □expressing CD41a and CD36 are depicted as red events in the upper□right quadrant, indicating a CD36-positive platelet subpopulation at 1.89% of the gated platelets. Bottom-left panel: Histogram illustrating CD36 fluorescence intensity across the gated platelet population. The mean fluorescence intensity (MFI) threshold defining CD36 positivity exceeds 10 (Log scale), consistent with established gating criteria used in quantitative assays of platelet CD36 expression. This threshold distinguishes CD36-deficient and CD36-expressing platelets, as commonly applied in clinical flow cytometry analyses.

(B) Platelet IgM binding (PSP-M2(D1)-IgM). Top-left panel: Dot plot showing PerCP□conjugated Mouse Anti□Human CD41a fluorescence intensity (X-axis) versus forward scatter (cell size, Y-axis). The rectangular gate isolates the platelet population, leveraging platelet-specific CD41a expression and size characteristics to ensure accurate identification. Top-right panel: Two-parameter dot plot of FITC-conjugated IgM (X-axis) versus PerCP-conjugated CD41a (Y-axis). Platelets □expressing CD41a and IgM are depicted as red events in the upper□right quadrant, indicating a minimal IgM-positive platelet subpopulation at 0.04% of the gated platelets. Bottom-left panel: Histogram illustrating IgM fluorescence intensity across the gated platelet population. The MFI threshold defining IgM positivity exceeds 10 (Log scale), which aligns with accepted gating standards. The low positive event count supports this sample's rarity of IgM surface binding. FITC-conjugated IgM (Isotype Control) is used to set the negative fluorescence intensity and is as the negative control.

(C) Monocyte CD36 expression (WB-M2(D1)-CD36). Top-left panel: Dot plot showing PerCP□conjugated Mouse Anti□Human CD14 fluorescence intensity (X-axis) versus forward scatter (cell size, Y-axis). The rectangular gate isolates the monocyte population, leveraging CD14 expression and size characteristics for accurate identification. Top-right panel: Two-parameter dot plot of FITC-conjugated Mouse Anti-Human CD36 (X-axis) versus PerCP-conjugated CD14 (Y-axis). In the upper right quadrant, Monocytes co□expressing CD14 and CD36 are depicted as red events, indicating a CD36-positive monocyte subpopulation at 1.54% of the gated monocytes. Bottom-left panel: Histogram illustrating CD36 fluorescence intensity across the gated monocyte population. The MFI threshold defining CD36 positivity exceeds 100 (Log scale), enabling the differentiation of CD36-deficient from CD36-expressing monocytes, consistent with clinical flow cytometry gating standards.

(D) Monocyte IgM binding (WB-M2(D1)-IgM). Top-left panel: Dot plot showing PerCP□conjugated Mouse Anti□Human CD14 fluorescence intensity (X-axis) versus forward scatter (cell size, Y-axis). The rectangular gate isolates the monocyte population, leveraging CD14 expression and size characteristics for accurate identification. Top-right panel: Two-parameter dot plot of FITC-conjugated IgM (X-axis) versus PerCP-conjugated CD14 (Y-axis). Monocytes co□expressing CD14 and IgM are depicted as red events in the upper□right quadrant, indicating a small IgM-positive monocyte subpopulation at 0.70% of

the gated monocytes. Bottom-left panel: Histogram illustrating IgM fluorescence intensity across the gated monocyte population. The MFI threshold defining IgM positivity exceeds 10 (Log scale), consistent with established clinical flow cytometry gating criteria. The low positive percentage suggests minimal IgM surface binding. FITC-conjugated IgM (Isotype Control) is used to set the negative fluorescence intensity and is as the negative control.

(E) Molecular Characterization of CD36 Deficiency: Identification of Pathogenic Variants by Sanger Sequencing. This figure illustrates representative gene sequencing chromatograms from patients diagnosed with type I CD36 deficiency, highlighting distinct pathogenic variants across exon 5 of the CD36 gene. The panel presents a frameshift mutation (c.329_330delAC) (rs572295823)in exon 5, introducing a premature shift in the reading frame at amino acid 110, predicted to generate a truncated, non-functional protein.

Figure 7

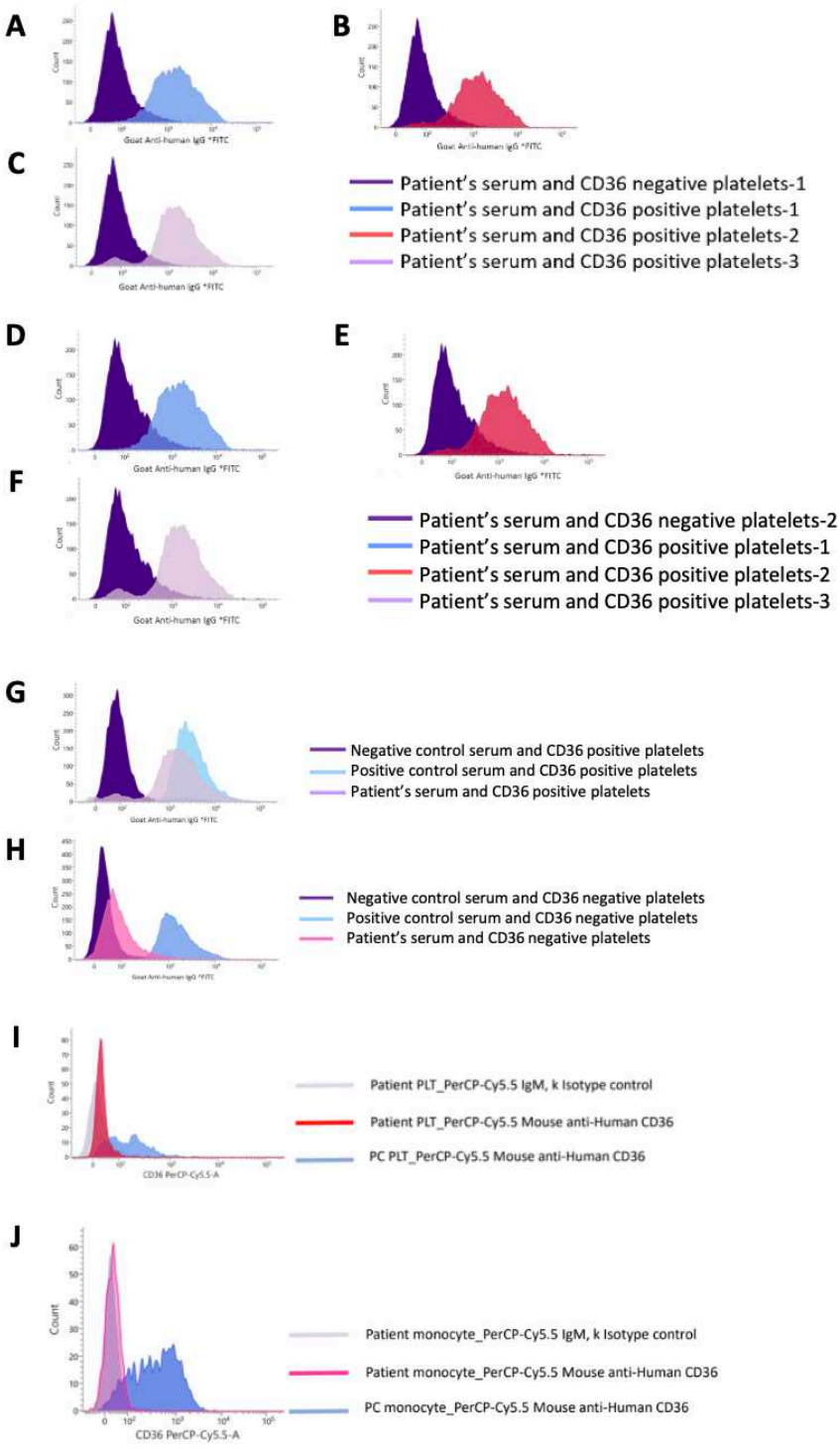

Figure 7

Flow Cytometric Confirmation of Type I CD36 Deficiency and Anti-CD36 Alloantibody Detection Shows absence of CD36 expression on patient platelets and monocytes, coupled with specific anti-CD36 IgG binding on CD36-positive targets, confirming type I CD36 deficiency and alloimmunization.

(A-C) Flow cytometric analysis of CD36 antigen expression on patient blood cells. Peripheral blood samples were analyzed using PerCP-Cy5.5–conjugated goat anti-human CD36 antibody and matched isotype controls. Flow cytometry shows absent CD36 expression on both platelets and monocytes, confirmed using PerCP-Cy5.5–conjugated anti-CD36 antibody and matched isotype controls. Positive control monocytes from a healthy donor validate assay specificity.

(D-F) Patient and control sera were incubated separately with CD36-negative and CD36-positive platelet targets, followed by FITC-conjugated goat anti-human IgG. **(D) Patient serum + CD36– platelets:** Histogram overlay of FITC fluorescence for CD36– platelets incubated with patient serum (blue) versus negative control serum (purple) shows only background binding. **(E) Patient serum + CD36+ platelets:**Corresponding overlay for CD36+ platelets revealed a marked rightward shift with patient serum (red), indicating specific anti-CD36 IgG binding; negative control serum (purple) remains at background. **(F) Positive control serum + CD36+ platelets:** FITC fluorescence of CD36+ platelets incubated with patient serum (pink) exhibits a similar rightward shift relative to negative control (purple), confirming assay sensitivity and specificity.

(G-H) Platelet Immunofluorescence Assay (PIFA) Confirms Anti-CD36 Antibody Binding. Immunofluorescence images demonstrate specific binding of anti-CD36 antibodies from patient and positive control sera to CD36-positive platelets, with no reactivity on CD36-negative targets, validating assay specificity. **(I-J)** Differential CD36 Expression in Platelets and Monocytes by Flow Cytometry. The panels demonstrate absent CD36 expression on both patient platelets and monocytes. These findings are consistent with a **CD36-deficiency type I** phenotype.